PUBLISHED VERSION

David A. Foster and Ben D. Goscombe
Continental growth and recycling in convergent orogens with large turbidite fans on oceanic crust
Geosciences, 2013; 3(3):354-388

Originally published at:
http://doi.org/10.3390/geosciences3030354

Geosciences **2013**, *3*, 354-388; doi:10.3390/geosciences3030354

OPEN ACCESS

geosciences

ISSN 2076-3263

www.mdpi.com/journal/geosciences

Review

Continental Growth and Recycling in Convergent Orogens with Large Turbidite Fans on Oceanic Crust

David A. Foster [1,*] and Ben D. Goscombe [2]

[1] Department of Geological Sciences, University of Florida, Gainesville, FL 32611, USA

[2] Integrated Terrane Analysis Research, 18 Cambridge Road, Aldgate, South Australia 5154, Australia; E-Mail: ben.goscombe@adelaide.edu.au

* Author to whom correspondence should be addressed; E-Mail: dafoster@ufl.edu; Tel.: +1-352-392-2231; Fax: +1-352-392-9294.

Received: 9 May 2013; in revised form: 13 June 2013 / Accepted: 14 June 2013 / Published: 5 July 2013

Abstract: Convergent plate margins where large turbidite fans with slivers of oceanic basement are accreted to continents represent important sites of continental crustal growth and recycling. Crust accreted in these settings is dominated by an upper layer of recycled crustal and arc detritus (turbidites) underlain by a layer of tectonically imbricated upper oceanic crust and/or thinned continental crust. When oceanic crust is converted to lower continental crust it represents a juvenile addition to the continental growth budget. This two-tiered accreted crust is often the same thickness as average continental crustal and is isostatically balanced near sea level. The Paleozoic Lachlan Orogen of eastern Australia is the archetypical example of a tubidite-dominated accretionary orogeny. The Neoproterozoic-Cambrian Damaran Orogen of SW Africa is similar to the Lachlan Orogen except that it was incorporated into Gondwana via a continent-continent collision. The Mesozoic Rangitatan Orogen of New Zealand illustrates the transition of convergent margin from a Lachlan-type to more typical accretionary wedge type orogen. The spatial and temporal variations in deformation, metamorphism, and magmatism across these orogens illustrate how large volumes of turbidite and their relict oceanic basement eventually become stable continental crust. The timing of deformation and metamorphism recorded in these rocks reflects the crustal thickening phase, whereas post-tectonic magmatism constrains the timing of chemical maturation and cratonization. Cratonization of continental crust is fostered because turbidites represent fertile sources for felsic magmatism. Recognition of similar orogens in the Proterozoic and Archean is important for the evaluation of crustal growth models, particularly for those based on detrital zircon

age patterns, because crustal growth by accretion of upper oceanic crust or mafic underplating does not readily result in the addition of voluminous zircon-bearing magmas at the time of accretion. This crust only produces significant zircon when and if it partially melts, which may occur long after accretion.

Keywords: continental growth; tectonics; turbidites; subduction; Gondwana; Damara Orogen; Lachlan Orogen; New Zealand

1. Introduction

The growth and evolution of continental crust through geological time is the result of a balance between the magmatic extraction of juvenile material from the mantle and the return of continental material to the mantle via sediment subduction, subduction erosion, and delamination. Continental growth occurs at plate boundaries and within plates via plumes, and the relative importance between these has changed over time. The record of continental growth remains elusive because orogenic processes often lead to significant recycling of continental material, and the record of juvenile material added to the crust is often not directly preserved (e.g., through detrital zircon ages).

Turbidite fan systems deposited on oceanic crust or within oceanic back-arc basins form the basis for constructing stable continental crust consisting of a mixture of juvenile mafic material from the asthenospheric mantle along with recycled continental detritus [1–3]. Turbidite-dominated orogens develop a layered crust with a mafic lower and felsic upper crust [2]. Turbidite-dominated orogens throughout geological time are variable mixtures of recycled continental and mantle-derived materials. Their recognition in the rock record depends on resolving the nature of the lower crust, sources of subduction/accretion related magmas, and provenance of the turbidites.

This paper summarizes the architecture of continental crustal formed by accretion of turbidite sequences using three examples. Controls on turbidite fan deformation and accretion include the plate tectonic setting, the tectonic position (either on the overriding plate or subducting plate), the degree of coupling between overriding and subducting plates that controls accretion *vs.* sediment subduction, the original thickness of the fan, the residence time of the fan on the seafloor, the degree of lithification (diagenesis/metamorphism), the depth of the lower-upper crust boundary in the accretionary wedge, the age of the oceanic basement, and the availability of fluids. Examples from the Cambrian Damara Orogen, Paleozoic Lachlan Orogen, and Mesozoic Rangitatan Orogen highlight the widely variable templates of turbidite-dominated orogens and their similarities using regional to meso-scale structures to delineate tectonic and magmatic evolution. We also discuss implications of accreted turbidite-dominated orogens as a crustal growth process in the Precambrian, as well as the lack of expression of these orogens in global detrital zircon U–Pb age distributions.

2. Orogen Architecture

The Neoproterozoic-Cambrian Damara Orogen in Namibia, the Paleozoic Lachlan Orogen of eastern Australia and the Mesozoic Rangitatan Orogen of New Zealand are examples of turbidite-dominated orogens within and along the margin of the Gondwanan supercontinent (Figure 1).

The Damara Orogen (Figure 2) is a doubly vergent orogen between the Congo and Kalahari cratons with thrusting of the carbonate platform and passive margin sequences to the north and south over the bounding cratons. The core is dominated by granitic batholiths and high-T/low-P metamorphism. The location of the felsic magmatism, as well as the structural asymmetry, reflects subduction dipping beneath attenuated Congo craton [4]. The Lachlan Orogen (Figure 2) is made up of an Ordovician oceanic volcanic arc, a high-T/low-P metamorphic complex, structurally thickened quartz-rich submarine fans and inverted Siluro-Devonian basins [2]. The Rangitatan Orogen of New Zealand (Figure 2) is made up of a structurally thickened sediment wedge abutting arc-forearc sequences and a deformed turbidite fan system (Torlesse of Rakaia wedge) separated by a steeply dipping, fault-bounded, ophiolite belt [5]. Structural vergence in the schists suggests NE thrusting of the trench volcaniclastic sedimentary sequence over a subducted quartz-rich sedimentary fan [6].

Figure 1. (**a**) Map of Gondwana at about 530 Ma showing the distribution of Precambrian cratons and Neoproterozoic, Paleozoic, Paleozoic-Mesozoic and Mesozoic-Cenozoic orogenic belts. The locations of schematic crustal profiles A–A′ (Lachlan), B–B′ (Damara) and C–C′ (Rangitatan) in Figure 2 are shown as solid lines (modified from Foster and Gray [2]). SF—Sao Franscico; RP—Rio de la Plata; (**b**) Map showing the timing of accretion of oceanic successions along the Australia and Antarctica segment of the East Gondwana margin. Map modified from Veevers [7].

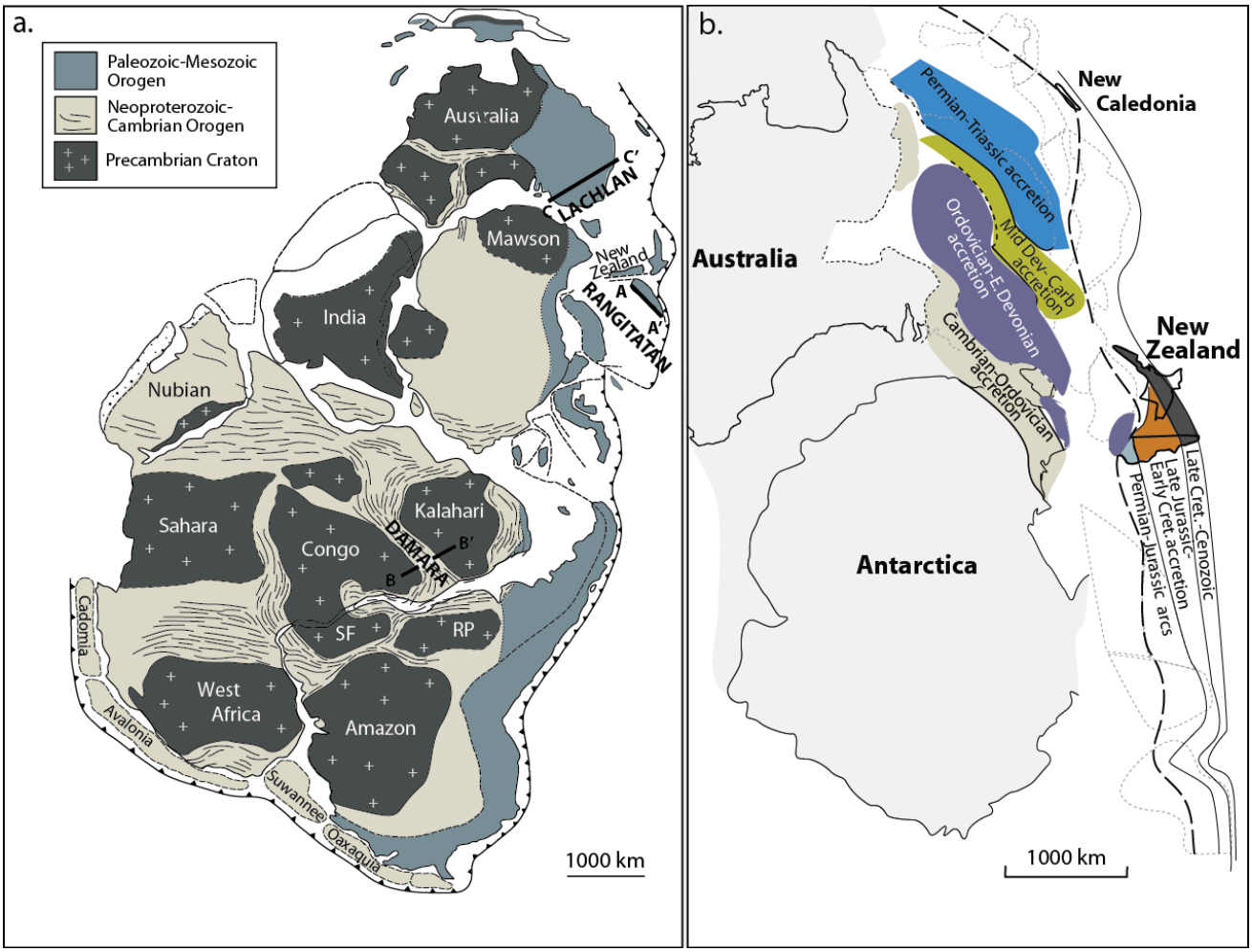

Figure 2. Schematic structural profiles across the Lachlan, Rangitatan, and Damara orogens showing the locations of turbidites with respect to other tectonic and elements.

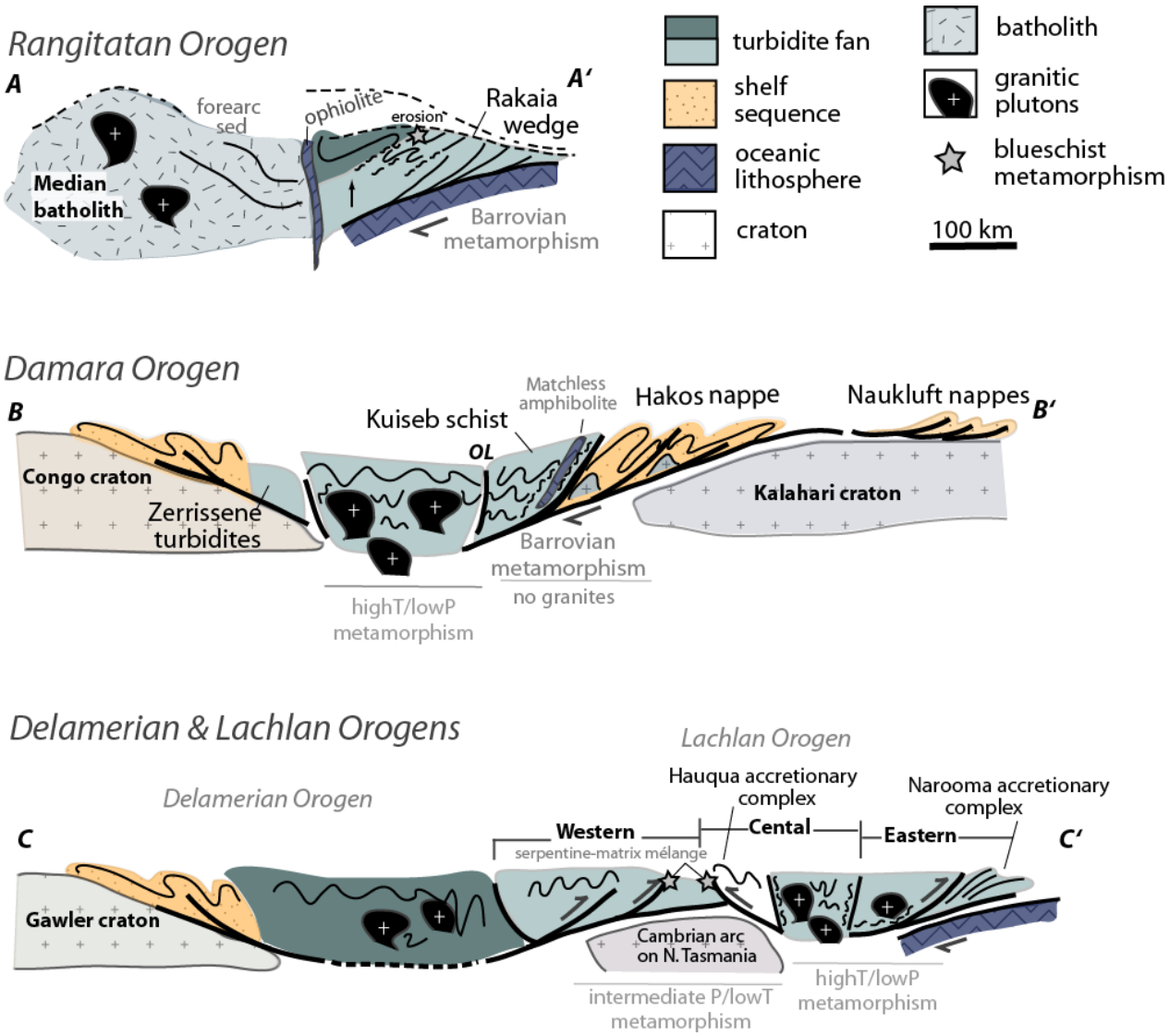

2.1. The Lachlan Orogen, Australia

The Paleozoic Lachlan Orogen is a composite accretionary orogen that forms part of the Paleozoic Tasman orogenic system of the eastern Australia and Gondwana (Figures 1 and 3) [2,8,9]. The Lachlan Orogen is dominated by Cambrian and Ordovician turbidites that formed a large submarine fan system comparable in size to the Bengal fan [10]. On the basis of paleocurrent information, the U–Pb ages of detrital zircons $^{40}Ar/^{39}Ar$ ages of detrital muscovites, and Nd–Sm whole rock isotopic data, the quartz-rich turbidites and black shales were sourced mainly from the Cambrian Delamerian-Ross Orogen along the margin of Gondwana and other Pan-African aged orogenic belts [7,11–15]. The detrital zircon U–Pb data are summarized in figure 128 of Veevers [7]. The turbidite fan accumulated on Middle to Late Cambrian backarc and forearc crust, consisting predominantly of MORB- to arc-tholeiitic basalt, gabbro, boninite, ultramafic rocks, and calc-alkaline arc rocks [16–18]. Closure of the Lachlan back-arc basin took place from ~450 Ma through 340 Ma, with accretion of

structurally-thickened submarine fans, accretionary complexes, extinct volcanic arcs, oceanic crust, and the Tasmanian microcontinent [2,9,18,19].

Figure 3. Tectonic map of Australia showing tectonic subdivisions and the major structural elements.

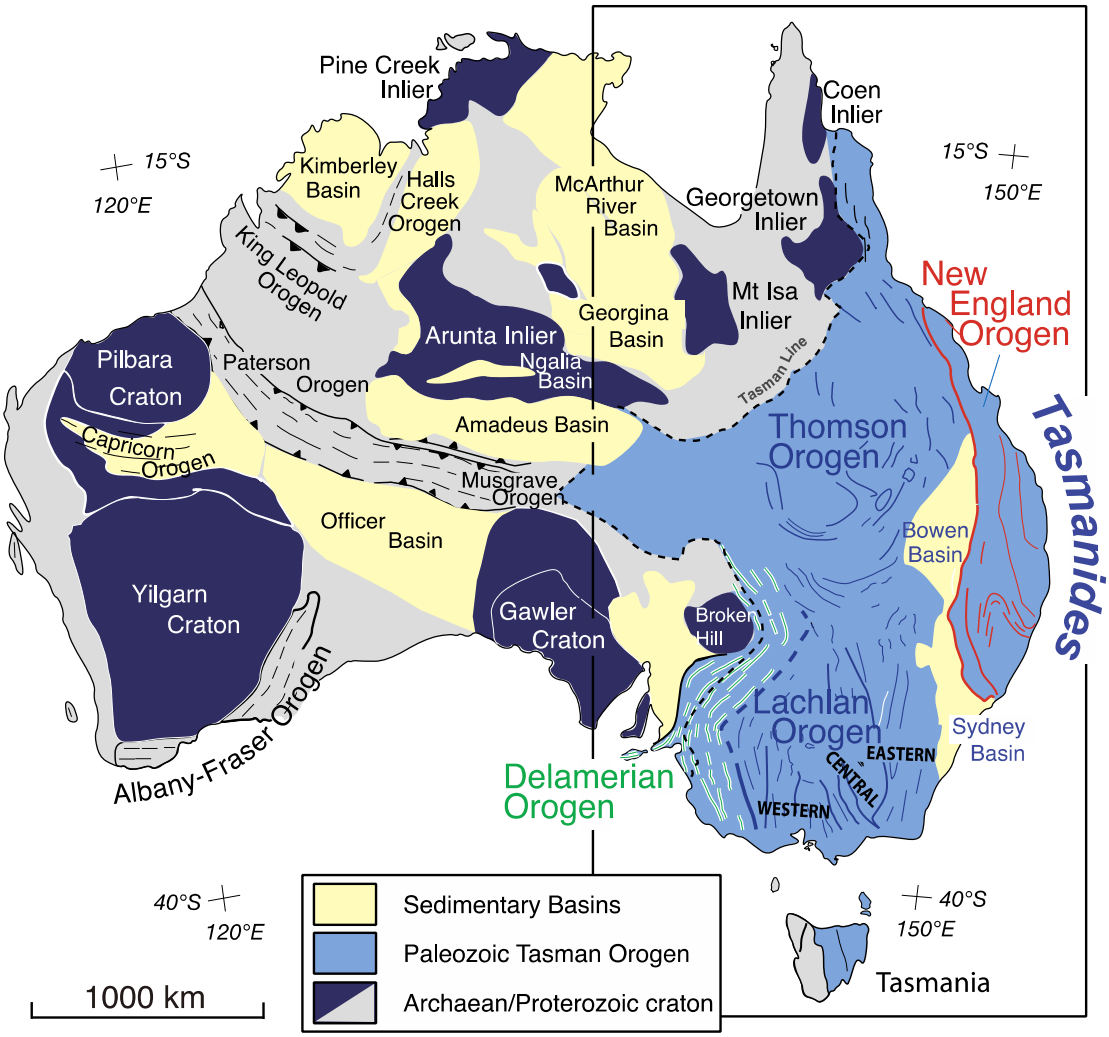

The Lachlan Orogen comprises three thrust-belts that constitute the western, central and eastern parts, respectively (Figures 3 and 4). The western Lachlan (WLO) consists largely of an east-vergent thrust system (Figure 5). The central Lachlan (CLO) is dominated by northwest-trending structures and consists of a southwest-vergent thrust-belt (Howqua accretionary complex) linked to a high-T/low-P metamorphic complex. The eastern Lachlan (ELO) is dominated by north-south trending structures and east-directed thrust faults; in the easternmost part an east-vergent thrust system overrides an older, subduction-accretionary complex (Narooma accretionary complex). Shortening via under-thrusting of the back-arc lithosphere for the WLO and CLO is suggested by the presence of dismembered ophiolite slivers along major fault zones [20], the low-T/intermediate-P metamorphism of meta-sandstone/slate sequences of the WLO and external part of the CLO [21,22], the presence of broken formation in the CLO and ELO [23–25], and a serpentinite-matrix mélange incorporating blueschist blocks [26,27].

Figure 4. Map of eastern Australia showing the major lithofacies and tectonostratigraphic elements (modified from Gray and Foster [8]).

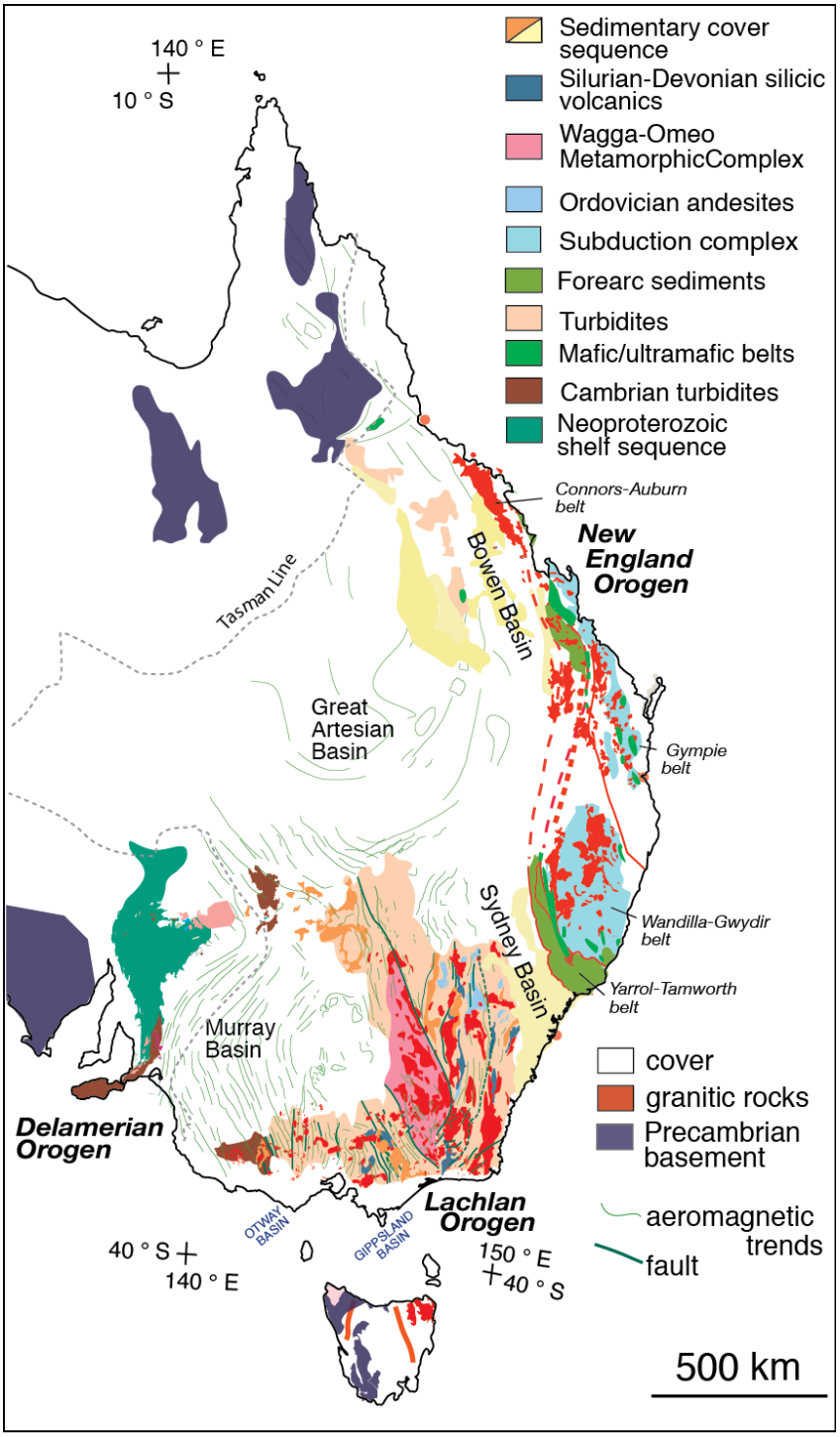

The turbidite successions of the Lachlan Orogen are generally metamorphosed to greenschist and subgreenschist (anchizonal) conditions (Figure 6b). Most of the turbidites are within the chlorite zone with localized biotite zone conditions in contact aureoles around granitoids. Exceptions include low-P/high-T migmatites and K-feldspar-cordierite-sillimanite gneisses (700 °C and 3–4 kbar) in the Wagga-Omeo Complex and the Eastern Metamorphic belt. These high-T belts are intimately associated with S-type granitic plutons and anatectic migmatites, and represent deeper parts of the orogenic pile exhumed during extension [28,29].

Figure 5. Composite structural profile across the southern Tasmanides at about 37.5° south latitude (see Gray *et al*. [30] for locations of segments).

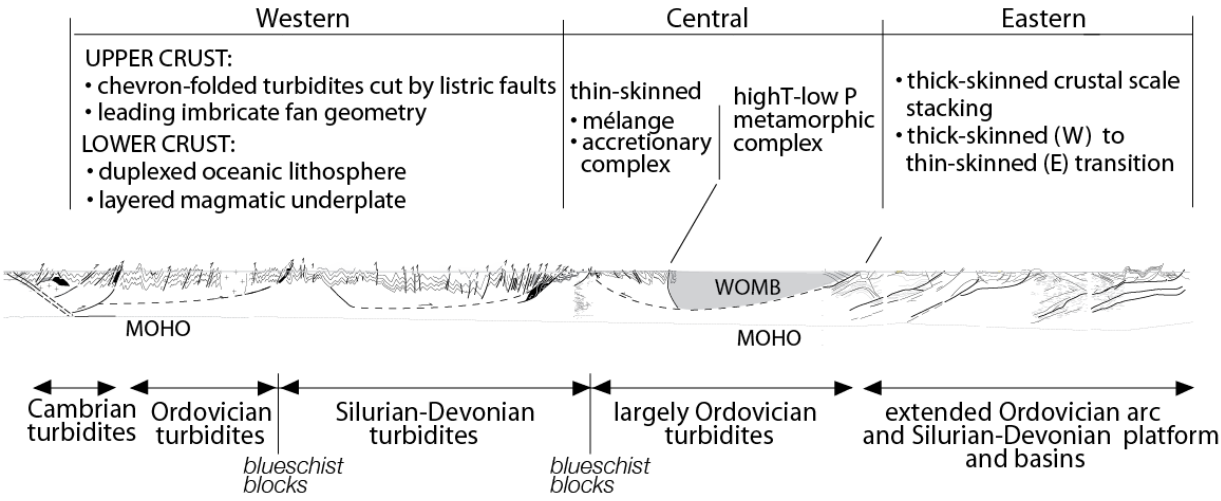

Figure 6. (**a**) Map showing the major tectonic elements of the Lachlan Orogen (after Gray and Foster [19]). The bold lines show locations of major faults and the finer gray lines show the orientation of the major structural grain; (**b**) Map showing the average grade of regional metamorphism across the Lachlan (after Gray and Foster [19]). Eastern Metamorphic complex abbreviations: CMC-Cooma, CaMC-Cambalong, JMC-Jerangle and KMC-Kuark; (**c**) Map showing the age and location of major Paleozoic granitic plutons in the Lachlan (after Foster and Gray [2]); (**d**) Map showing the age of major deformation and metamorphism for different locations across the Lachlan (after Foster and others [31]). White arrows indicate the trend direction of younger deformation.

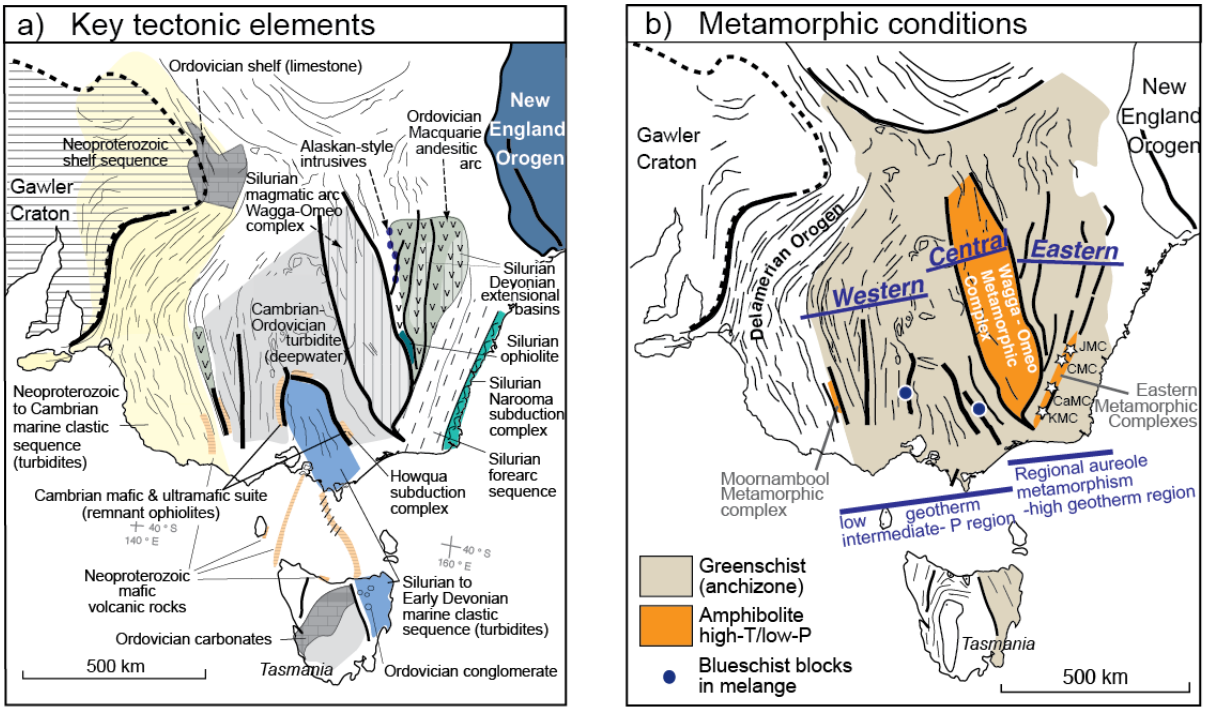

Figure 6. *Cont.*

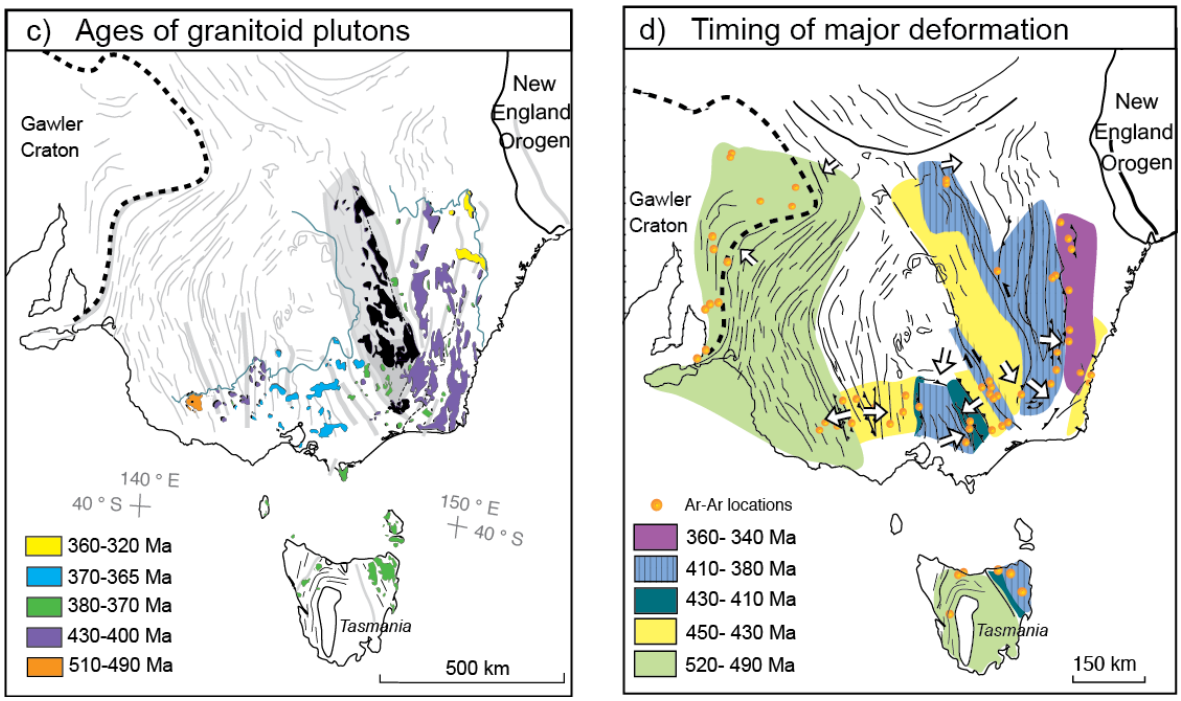

Turbidites from the low-grade parts of the Lachlan Orogen show intermediate pressure series metamorphism based on b_0 values of phengitic micas and chlorite-actinolite assemblages in metabasites [19,21], as well as intermediate-P/low-T blueschist metamorphism (6–7 kbar, <450 °C) of metabasaltic blocks in serpentinite/talc-matrix mélanges [26,27]. The intermediate-P/low-T metamorphism occurred at 450–440 Ma during the regional deformation of the Lachlan Orogen [26,27,32].

Silurian-Devonian granitic rocks form about 20% of the present outcrop in the Lachlan Orogen (Figure 6) [33,34]. Most of the granitic plutons crystallized at about 2 kbar pressure or less and intrude low-grade metamorphic rocks. The majority are post-tectonic and unmetamorphosed, although the older intrusions (Wagga-Omeo Belt, Kosciusko Batholith) are strongly deformed and were emplaced syn- to late-kinematically and at mid-crustal depths [35,36]. Volcanic sequences, mostly dacite-rhyolite, are also widespread (15% of area in eastern Lachlan Orogen, significant caldera complexes in western Lachlan Orogen) and associated with shallow granitic plutons. Basaltic to andesitic volcanic rocks comprise the Ordovician (480–460 Ma) Macquarie Arc in the eastern Lachlan Orogen [37,38]. Excluding the Macquarie Arc, the Lachlan Orogen igneous rocks range from about 430 to 370 Ma, with broad west-to-east younging trends in the eastern (430–370 Ma) and western (410–370 Ma) belts, respectively. Carboniferous (*ca.* 320 Ma) granites occur along the eastern edge of the Lachlan Orogen [34].

S-type granitoids make up about half of the exposed granitic plutons in the Lachlan Orogen and are concentrated in a NNW-trending belt along the center of the orogen. Compositions range from Mg-Fe-rich cordierite-bearing granodiorite [34,35] to highly fractionated granite [39]. Felsic S-type granites (410–370 Ma) also occur in the WLO; the youngest (370 Ma) intrusions are associated with extensive caldera complexes [40–42]. I-type granites form a broad belt in the eastern Lachlan (e.g., 8620 km^2, 419–370 Ma, Bega Batholith), but are also abundant throughout the rest of the orogen. Medium-to high-K granodiorites and granites dominate, with lesser tonalite and rare diorite and gabbro.

Trace element patterns in I- and S-types are typically similar and display low Sr/Y ratios. A-type granitic rocks are uncommon and tend to be post-orogenic [43]. Sr and Nd isotopic data ($^{87}Sr/^{86}Sr$ 0.704 to 0.720; εNd +4 to −11 [44,45]) define a hyperbolic mixing array. I-type granites generally give lower $^{87}Sr/^{86}Sr$ and higher εNd than S-types, which trend towards the more evolved compositions of the Paleozoic turbidites ($^{87}Sr/^{86}Sr$ 0.715–0.730, εNd −8 to −12 [46]. Whole rock oxygen isotopes in the I-type (7.9‰–10‰) and S-type (9.2‰–12‰) granites of the eastern Lachlan Orogen show correlations with Sr and Nd isotopic ratios, consistent with mixing of high-$\delta^{18}O$ crustal and low-$\delta^{18}O$ mantle-derived components [44]. Lu–Hf isotopic data from igneous zircons range from εHf > +10 to <−10 with A- and I-types giving higher positive values, approaching depleted mantle, and S-types tending to give more negative values. The εHf values are correlated with $\delta^{18}O$ values of the zircons and whole rock Nd data, such that the positive εHf values correspond to more mantle-like $\delta^{18}O$ values and the strongly negative εHf zircon to $\delta^{18}O$ values of 8–11 [3,47].

The S-type granites contain zircon xenocrysts that give U–Pb age distributions dominated by *ca.* 500 and *ca.* 1000 Ma grains along with less abundant groups with ages as old as *ca.* 3.6 Ga [36,48,49]. The xenocrystic zircon age distributions are identical to detrital zircon age distributions in the Early Paleozoic turbidites [7], suggesting magma sources at least partly within the early Paleozoic meta-turbidites. Zircon inheritance in I-type granites is typically limited, but with the same age distribution as in the S-type granites [48], indicating a recycled sedimentary component was involved in the petrogenesis of I-types.

Mafic dikes, intrusions, and lavas across the Lachlan Orogen show signatures suggesting derivation as back-arc to arc mantle partial melts [49,50]. This suggests that the granites in the margin-parallel batholiths of the eastern/central Lachlan Orogen formed within arc/back-arc tectonic settings. The *ca.* 370 Ma post-orogenic magmatism in the western Lachlan Orogen is probably related to post-collision lithospheric delamination [51,52].

Silurian-Devonian igneous rocks of the Lachlan Orogen were, therefore, derived from a mixture of source components from depleted mantle, either directly or via partial melts of mafic crust, and partial melts of the turbidites [3,53–56]. The highest proportions of mantle-derived magmas are found in the post-orogenic A-types, which formed during extension and slab roll back [3]. The I-types are variable mixtures with greater proportions of mantle-derived magma than the S-types. This indicates that significant new crustal growth via mantle partial melting occurred during the extensional phases of the orogenic cycle, with variable amounts of growth and recycling occurring during shortening phases [3].

Tectonic Evolution

Extensive turbidite fan deposition took place in a marginal (back-arc) basin system (proto-Lachlan basin) on the Gondwana margin between ~490 Ma and 470 Ma (Figure 7a), with large turbidite fans spreading out onto Cambrian oceanic crust [19,57]. Turbidite deposition occurred at the same time that post-orogenic magmatism, cooling, and erosional exhumation occurred in the older Delamerian-Ross Orogen (~490–460 Ma; [15]). Outboard, subduction-related arc volcanism initiated prior to ~485 Ma in the oceanic plate forming the Macquarie magmatic arc [37] some thousands of kilometers from the Gondwanan margin [58] (Figure 7a).

Figure 7. Plate tectonic setting during the development and closure of the Lachlan backarc basin, and events leading to the accretion of the Lachlan Orogen. Red dots depict felsic pluton intrusion.

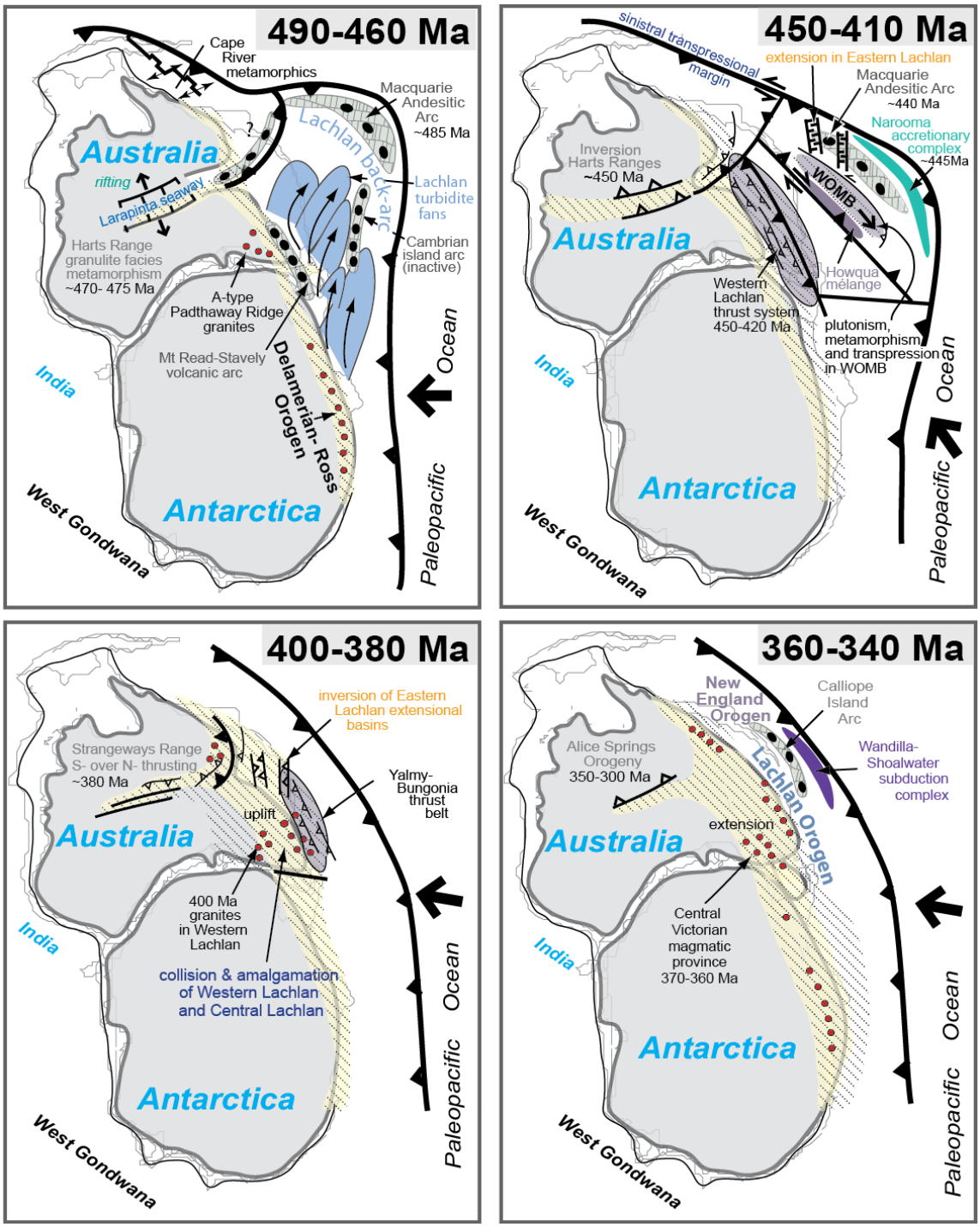

After 460 Ma the back-arc basin system began to close by subduction [31,59] inboard of the main Gondwanan subduction zone. Multiple oceanic thrust-systems operated in both the eastern and western parts of the basin at the same time (Figures 7b and 8a,b). Shortening of the basin, thickened and duplexed the oceanic crust and caused thrusting and chevron folding in the overlying turbidite wedge [60].

Figure 8. Tectonic evolution diagram illustrating the sequential construction of the crustal in the Lachlan Orogen.

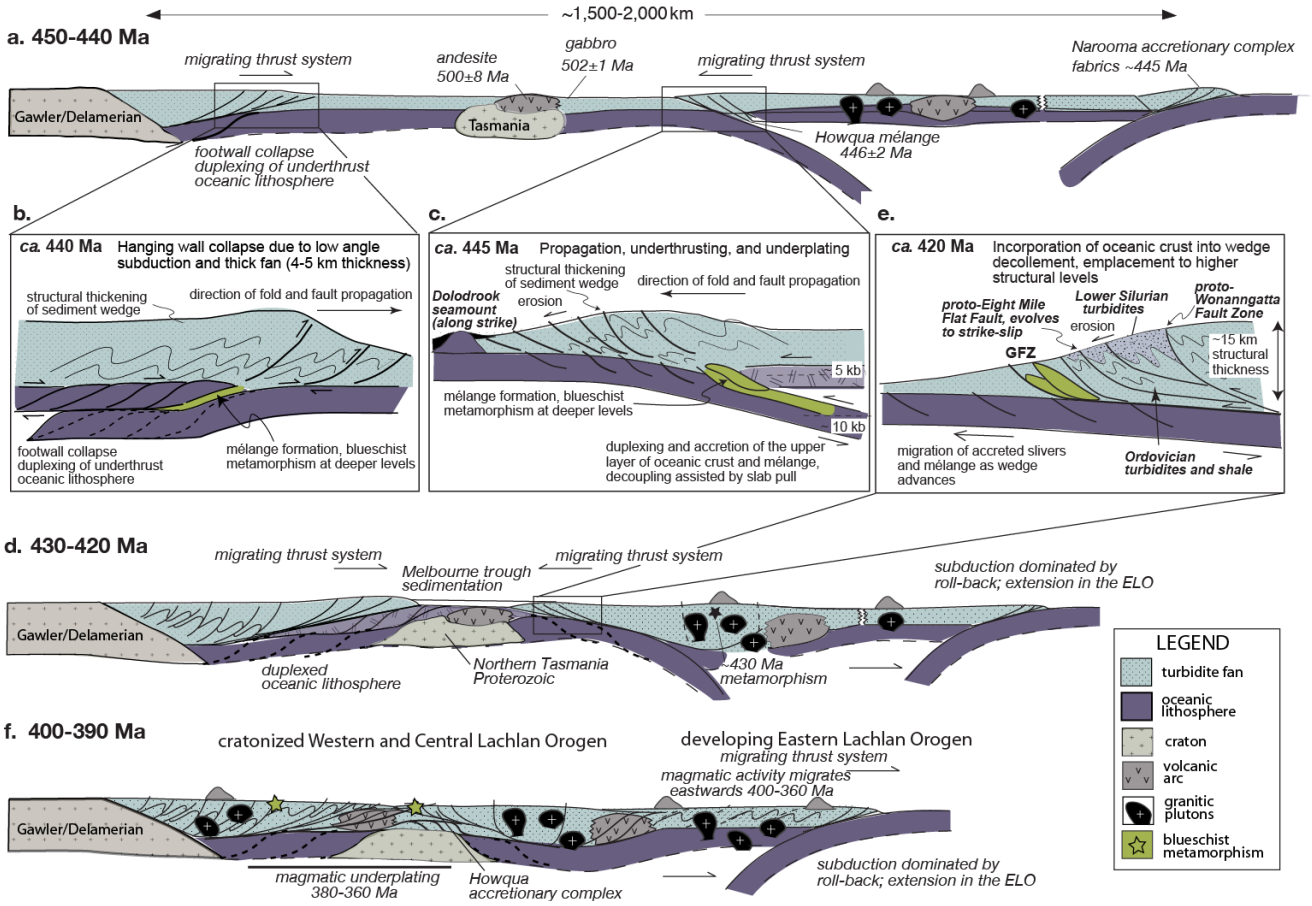

Widespread magmatism in the western part of the WLO at ~400 Ma was followed by final closure of the marginal basin, which was thrust over the northeastern part of the Tasmanian microcontinent by about 390 Ma (Figure 8f). Structural thickening and amalgamation of the WLO and CLO led to cratonization of the inner Lachlan [2]. Outboard in the ELO, syn-deformational *ca.* 440–435 Ma magmatism and high-T/low-P metamorphic belts formed during intermittent east-directed thrusting and periods of extension-related volcanism, particularly at *ca.* 420 Ma [61]. Post-orogenic silicic magmatism in the WLO (central Victorian magmatic province) occurred at *ca.* 370–360 Ma, while east-directed thrusting in the ELO caused inversion of former extensional basin faults, and was also followed by post-orogenic magmatism. The late stage magmatism may have been in response to partial removal of mantle lithosphere after closure of the back-arc-basin [51] or slab roll-back, which started a new cycle of extension and basin formation along the Gondwana margin [61]. The Lachlan Orogen was fully accreted to Gondwana by *ca.* 330 Ma.

2.2. The Rangitatan Orogen (Rakaia Wedge), New Zealand

The Rangitatan Orogen (Figure 1) is a collage of accreted arc and forearc assemblages, and a turbidite-dominated sediment wedge (Rakaia Wedge) that formed along the margin of Gondwana in Jurassic and Cretaceous times [6,62,63]. The Permian to Jurassic Torless turbidites were deposited on oceanic crust along the Gondwana margin and have detrital zircon U–Pb and detrital mica $^{40}Ar/^{39}Ar$

age distributions consistent with provenance in the New England Orogen of eastern Australia [64,65]. Deformation of the Rakaia wedge and its accretion to Mesozoic arcs and margin of Gondwana occurred when the oceanic plate carrying the thick turbidite succession was subducted.

The sediment wedge is made up of two distinct structural domains (Figure 9): (1) the Otago Schist belt characterized by schistosity and transposed layering at the mesoscale, and shear zones and recumbent isoclinal fold-nappes at the regional scale [6,66]; and (2) chevron folded younger sediments of the Pahau terrane [63]. The Permian Dun Mountain ophiolite and Maitai mélange form a steeply N-dipping boundary between the gently folded, arc and forearc sequences (Median Batholith, Brook Street and Murihiku terranes) to the south, and the deformed submarine fan sediments of the Torlesse composite-terrane to the north (Figure 9) [67,68]. The Torlesse composite terrane includes a crustal section composed of structurally thickened (~20 km thickness) Permian to Triassic-Jurassic sediments of the Rakaia terrane, structurally overlain by a ~10 km thick wedge of trench sediments (Caples terrane) immediately adjacent to the Livingstone fault [69]. In the hanging wall to the Livingstone fault, intensely-deformed monotonous quartzo-feldspathic schist, with minor intercalated micaceous schist, greenschist, and metachert (Otago Schist), occupies a domal culmination with a maximum subsurface width of ~220 km and ~20 km of structural relief [6] (Figure 9). North of the Waihemo Fault, there is a transition into a tectonically imbricated and weakly metamorphosed Permian-Triassic greywacke sequence of the Rakaia (Older Torlesse) terrane. South of the Livingstone fault the crustal section is composed of a ~10–15 km thick succession of Murihiku terrane forearc sediments (Triassic to Jurassic volcanogenic sandstone, siltstone and tuff), overlying a ~10 km thick arc sequence of Brook Street terrane volcanic rocks (layered gabbro-ultramafic sequences, diorites and volcaniclastic sediments, which are the roots of a Permian intra-oceanic arc).

Figure 9. (**a**) Tectonic map of New Zealand (modified from Gray *et al*. [30]); (**b**) Geological profile showing the crustal architecture of the southern part of the South Island (based on Mortimer *et al*. [67]).

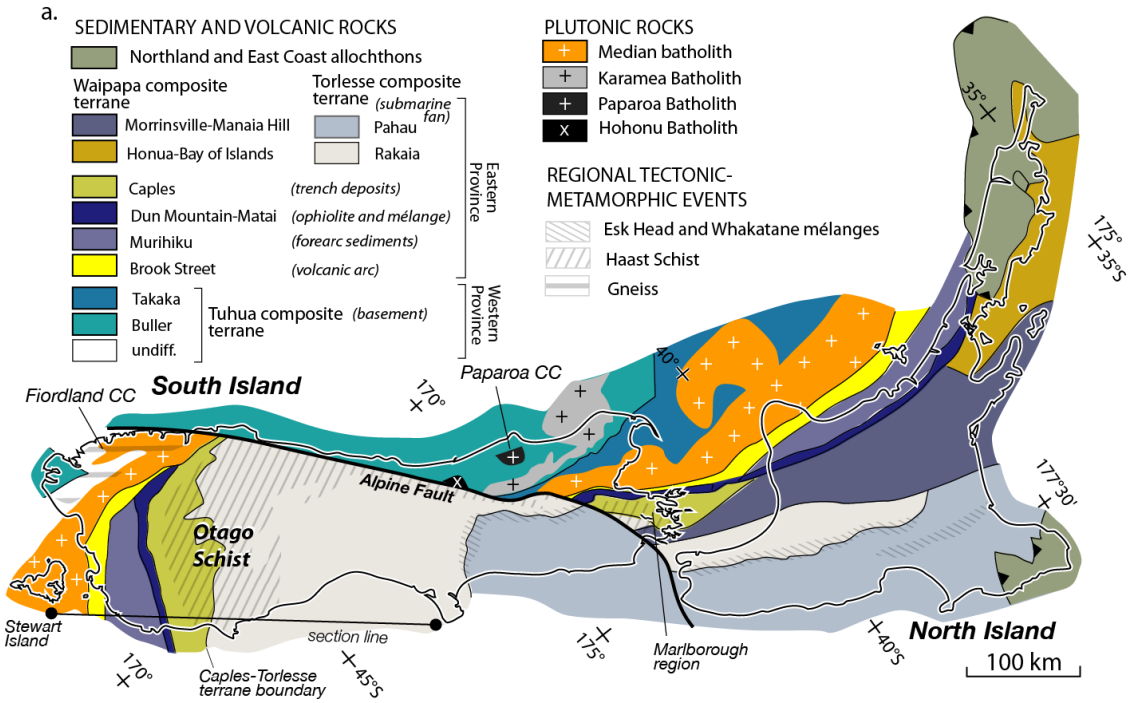

Figure 9. *Cont.*

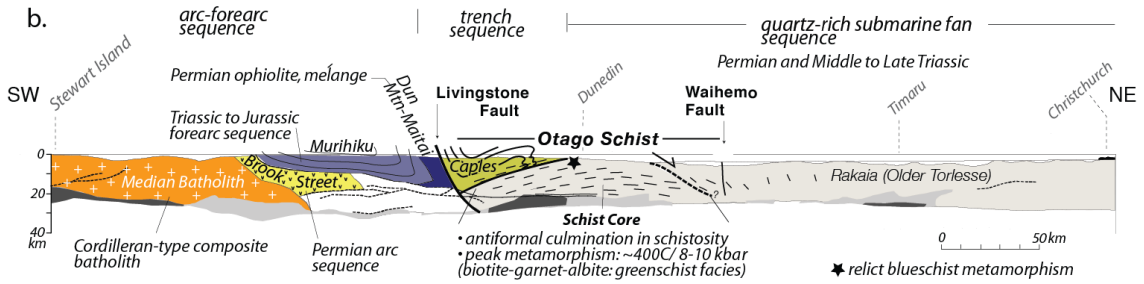

The Otago Schist belt is the metamorphosed part of the Rakaia wedge. Prehnite-pumpellyite facies rocks on the northern and southern flanks (Torlesse and Caples Terranes respectively) increase to upper greenschist facies, and then to epidote-amphibolite facies in the broad central portion [6,70]. Mineral parageneses indicate peak P-T conditions of 450 °C and 8–10 kbar [70], suggesting burial to depths of ~20–30 km (moderate-high P/T metamorphic series). Relict blueschist assemblages occur in mafic greenschist/chert sequences close to the Caples-Torlesse boundary, indicating an earlier high-P/low-T metamorphism [71].

Subduction-related magmatism in the overriding Gondwana plate formed the Median batholith (Figure 10) [72]. Granitoids of the Median batholith, represent a semi-continuous (230–125 Ma) calc-alkaline, I-type suite, which shows very little evidence of crustal involvement ($^{87}Sr/^{86}Sr \approx 0.7037$; $\varepsilon Nd \approx +4$) [73–76]. Collision between the arc and the wedge is marked by the 124–111 Ma Separation Point suite (Figure 10) and lower crustal, 126–119 Ma, metadiorites and metagabbros of the Western Fiordland orthogneiss [75,77–80]. These sodic I-type suites span a wide range in SiO_2, and have high to very high Sr/Y ratios [78]. This adakite-like suite probably resulted from partial melting of mafic rocks in the lower crust and mantle of the arc after substantial thickening of the arc crust.

Figure 10. Metamorphic and granitoid age map of New Zealand based on data summarized in Gray *et al*. [30].

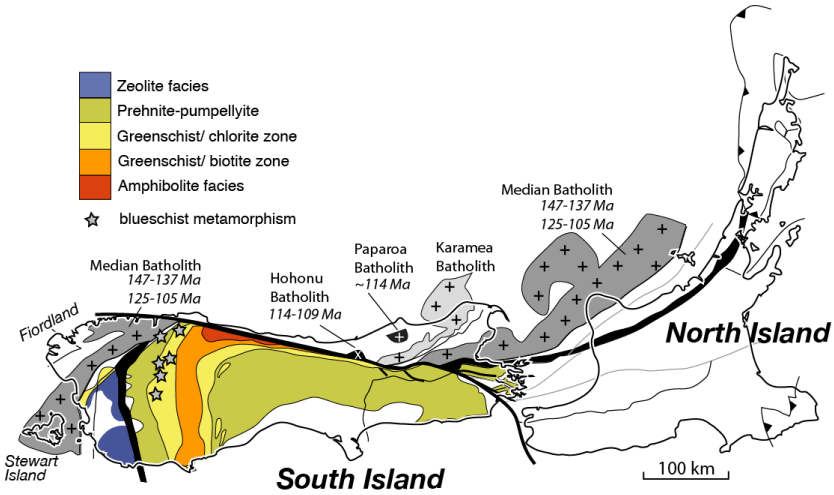

Granitic plutons coeval with the Rangitatan orogeny, therefore, occur within the Mesozoic arc (Median Tectonic Zone [81]) or along the Paleozoic Gondwanan margin and not within the accreted turbdites. These are almost all I-type plutons with weak or absent zircon inheritance and mantle-dominated Sr–Nd–O isotopic signatures. Partial melting of the exposed turbidites apparently did not occur during subduction accretion.

The youngest plutons in the belt are I- and S-type plutons in the Hohonu and Paparoa batholiths in NW South Island, which intrude Paleozoic Gondwana margin metasedimentary rocks. These plutons, known as the Rahu Suite, exhibit xenocrystic zircons (500–1000 Ma), more evolved radiogenic isotopic signatures than the older suite ($^{87}Sr/^{86}Sr$ 0.7062–0.7085, εNd ≈ −5), and elevated $\delta^{18}O$ [82,83], suggesting they are mixtures of partial melts of the Mesozoic arc crust and the older Paleozoic continental margin formed after the convergence switched to extension [83–85].

Tectonic Evolution

The Permian-Jurassic Torlesse fan with arc-forearc-trench slope sequences (Brook Street, Maitai, Murihiku and Caples terranes) formed in a convergent margin setting due to subduction of Permian oceanic crust beneath the Gondwana margin (Figure 11) [62,63,86]. Structural thickening of the Torlesse turbidite fan began in the Late Jurassic (~150–140 Ma), with Early Cretaceous (130–120 Ma) juxtaposition of Caples and deformed Torlesse sediment, and accretion of the turbidite fan to the margin [6,63,66]. This coincided with collision between the Median Tectonic Zone (Median Batholith) and the Gondwana margin, causing the onset of adakitic magmatism at 125–118 Ma [73,85].

Figure 11. Tectonic evolutionary diagrams illustrating the sequential stages in crustal accretion for New Zealand (modified from [30,62]).

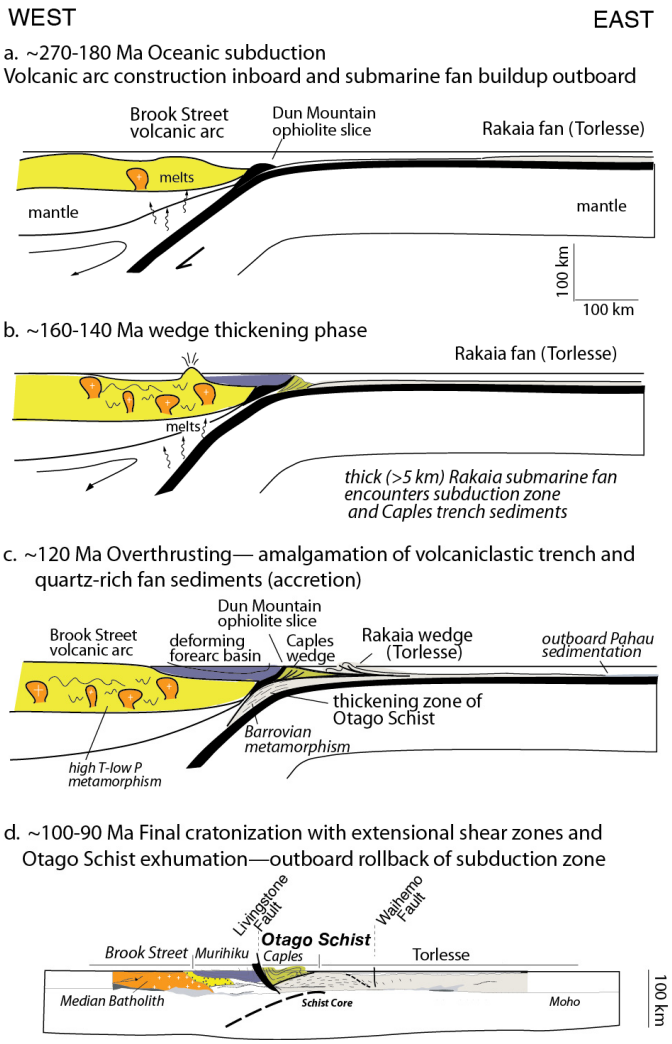

2.3. The Damara Orogen, Namibia

The Pan African Damara Orogen within Namibia consists of the Inland branch or Damara Belt, and Coastal branches comprising the Kaoko and Gariep Belts in the north and south, respectively (Figure 12) [86]. Metamorphosed turbidites make up a major component of the Damara Belt [30,86–90] and represent a Neoproterozoic submarine fan system and/or accretionary complex that formed in the Neoproterozoic Khomas ocean basin south of the Congo craton [91]. Detrital zircon U–Pb age distributions and Sm–Nd isotopic compositions of the Khomas tubidites indicate that they were sourced from Neoarchean to Cryogenian orogenic and magmatic components of the Congo craton (Figure 13).

Figure 12. (**a**) Simplified map of southern Africa showing the location of Mesoproterozoic-Archean cratons and the Damara Orogen; (**b**) Tectonic map of the Damara Orogen, Namibia and the location of the profile A–D in (Figure 13). (Map modified from Gray *et al*. [92]). NZ: Northern zone; CZ: Central zone; SZ: Southern zone; SMZ: Southern Margin zone; AF: Autseib Fault; OmSZ: Omaruru shear zone; OkSZ: Okahandja shear zone.

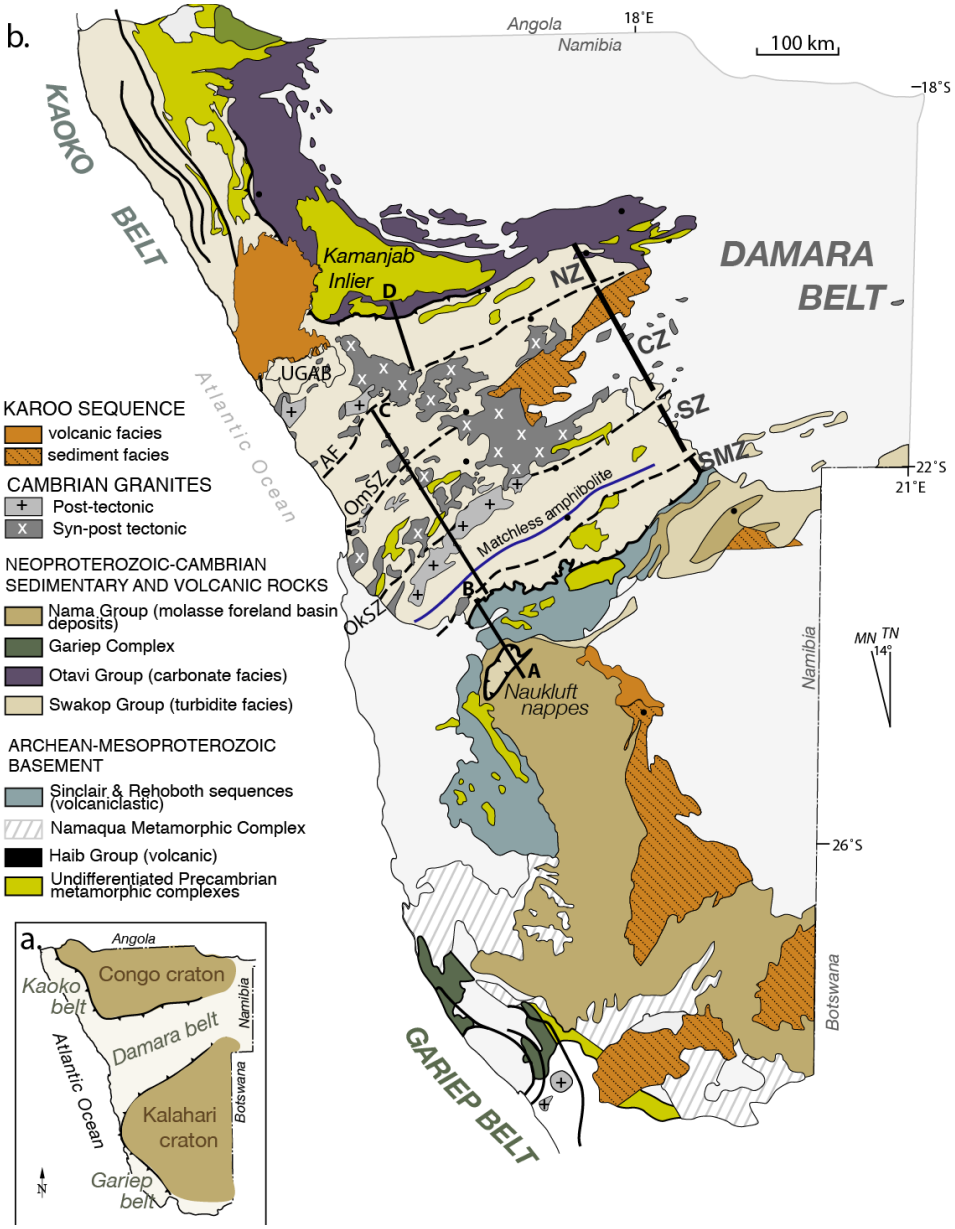

Figure 13. Composite kernel density estimation curve and histograms of detrital zircon U–Pb data from Kuiseb schist and related rocks of the Damara Supergroup in the core of the Damara Orogen (data from [92] Data shown are for U–Pb analyses that are <10% discordant: $^{207}Pb/^{206}Pb$ ages for analyses >1000 Ma, and $^{206}Pb/^{238}U$ ages are analyses <1000 Ma.

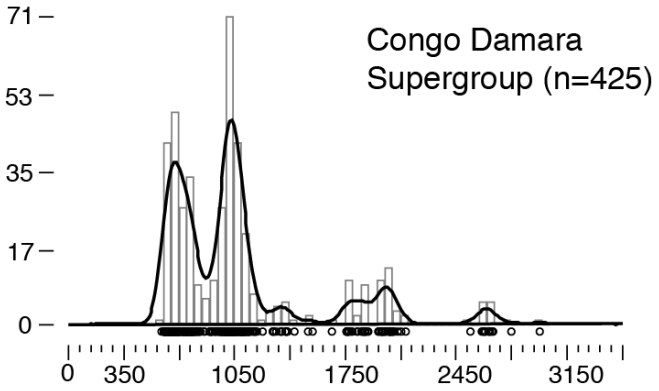

Khomas oceanic lithosphere is preserved in the thin (200–300 m thick) shear zone-hosted, Matchless amphibolite (Figure 12) [93]. This unit consists of intensely deformed basalt, pillow basalt, and gabbro with tholeiitic geochemistry [94], and intercalated with banded chert [95]. Widely separated serpentinite boudins within the Uis Pass Line shear zone at the margin between the accreted turbidite fan sequences and passive margin sequences of the Kalahari Craton mark the Khomas suture [93]. The flanks of the former ocean basin(s) are represented by two craton-verging thrust systems within shelf carbonates (Hakos and Naukluft nappes in the Southern Margin zone) [89].

The deep water Khomas turbidite sequence is metamorphosed to form the Kuiseb schist and subdivided into two structural-metamorphic zones, referred to as the Central and Southern zones (Figure 12). The Central zone is underlain by attenuated Congo craton [90,96], and underwent phases of low-P/high-T metamorphism and deformation (540–530 and 520–505 Ma) with voluminous granitic magmatism between 560 and 470 Ma (Figure 12) [92,97–102].

The thicker, deep-water sedimentary sequence experienced intermediate-P/intermediate-T (Barrovian) metamorphism and is now part of the ~100 km wide Southern zone [103,104]. This zone consists of homoclinally, N-dipping, Kuiseb Schist with transposed foliation and schistosity [89–91] that represents a major shear zone interface transitional into basement-cored fold- and thrust-nappes of the Southern Margin zone (Figure 14) [90,105]. U–Pb ages of metamorphic monazite suggest an age of 525–515 Ma for peak metamorphism in the Kuiseb Schist [104]. The western part of the Northern zone (Ugab domain) occurs at the transition between deep-water turbidite facies and slope-to-platform carbonates [106,107], and is intruded by *ca.* 530 Ma granites of the Central zone [101,105,107,108].

Figure 14. Geological profile showing the crustal architecture of the Damara Belt of the Damara Orogen (modified from Gray *et al*. [30] and references therein).

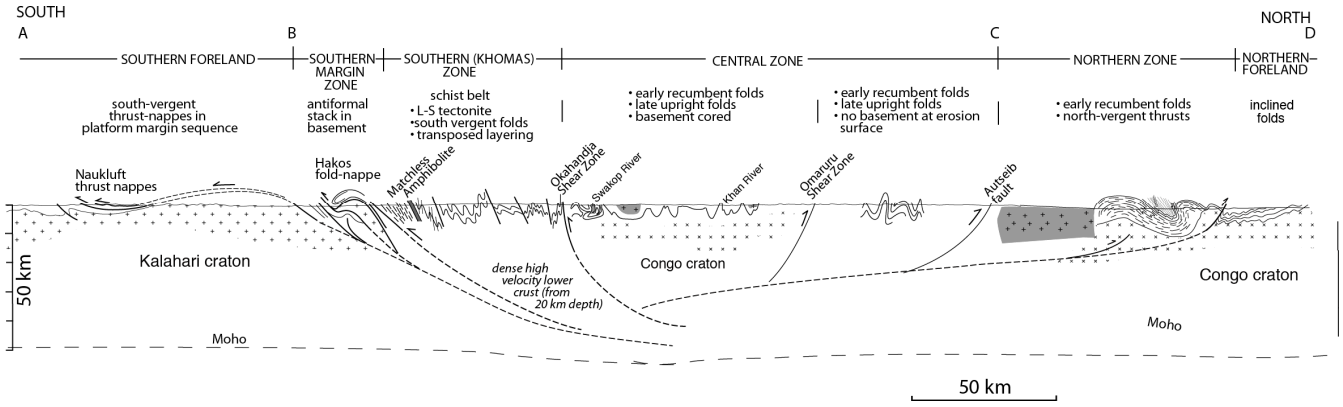

The Damara Belt exhibits elongated sections of intermediate-P/intermediate-T metamorphism and a low-P/high-T metamorphic core (Figure 15). Central zone metamorphism occurred under an elevated geothermal gradient (30–50 °C/km) with clockwise P-T paths [103,109] and includes garnet-cordierite granulites [110]. The Southern zone metamorphic conditions are moderate-P and T, with peak conditions of ~600 °C and ~10 kbar, but showing a decrease in pressure northwards to ~4 kbar near the Okahandja lineament [103]. The Southern zone has a low thermal gradient (18–22 °C/km), with syn-kinematic staurolite and syn- to post-kinematic garnet in metapelites defining a steep clockwise P-T path. The Northern zone shows high-P/moderate-T with a steep clockwise P-T path; peak conditions are estimated at 635 °C and 8–7 kbar and an average thermal gradient of 21 °C/ km [108].

Figure 15. Map of Cambrian metamorphism in the Damara Orogen compiled from sources listed in the text.

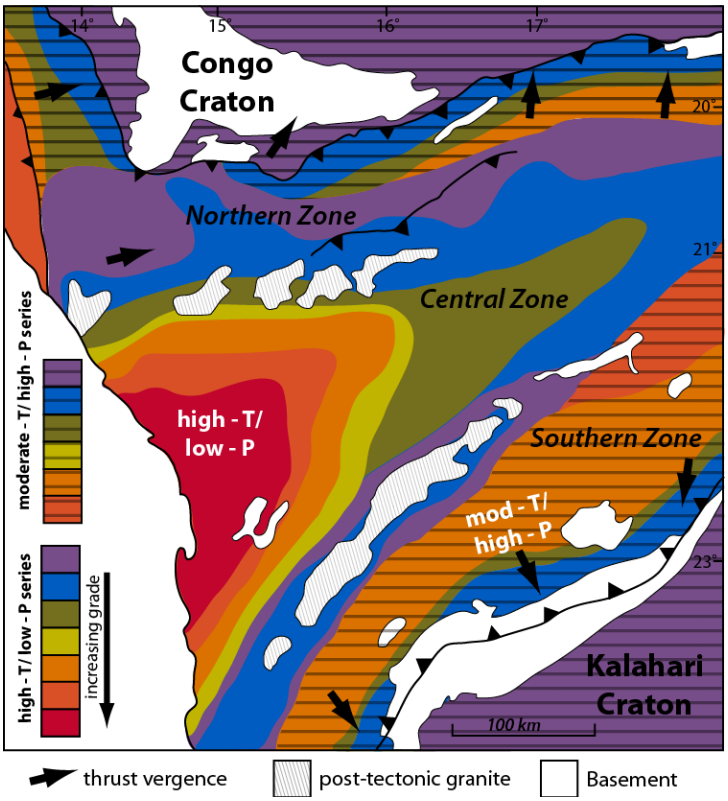

Granitic rocks comprise approximately 74,000 km^2, or roughly 25% of outcrop [90] of the Damara Belt. Most of the granitic magmatism was concentrated in the Central zone, with minor activity in the Northern zone; the post-tectonic Donkerhuk batholith (5000 km^2) is the only significant granitic complex in the Southern zone. McDermott *et al*. [111] divided the granitoids into 3 groups on the basis of geochemical signatures. Group 1 comprises peraluminous leucogranites and porphyritic, biotite-rich granite known as the "Salem-type" granites. Group 2 includes mildly peraluminous A-type granites with elevated high field strength element compositions (Nd–Zr–Y) compared to the other groups. Group 3 encompasses metaluminous calcalkaline quartz diorites and granodiorites.

Group-1 granites (96% of the exposed plutons) show a wide range of initial Sr and Nd whole-rock isotope ratios ($^{87}Sr/^{86}Sr$ 0.708–0.740, εNd −2 to −19 [111–114], reflecting involvement of Archean-Mesoproterozoic basement [114]. Many of the S-type granites give εNd values about −5, which are similar to Neoproterozoic (Swakop Group) turbidites (Figure 16) [113,115]. $\delta^{18}O$ values are typically 11‰–15‰, which is similar to both Damara metasediments and pre-Damara basement [100,116]. The elemental and isotopic data for the S-type granites indicate crustal sources within the Damara metasediments and/or pre-Damara basement, with dehydration partial melting at mid-crustal levels (>6 kb).

Figure 16. Histogram of Nd isotopic data (at the time of deposition) from Neoproterozoic peltic schists from the Damara Belt.

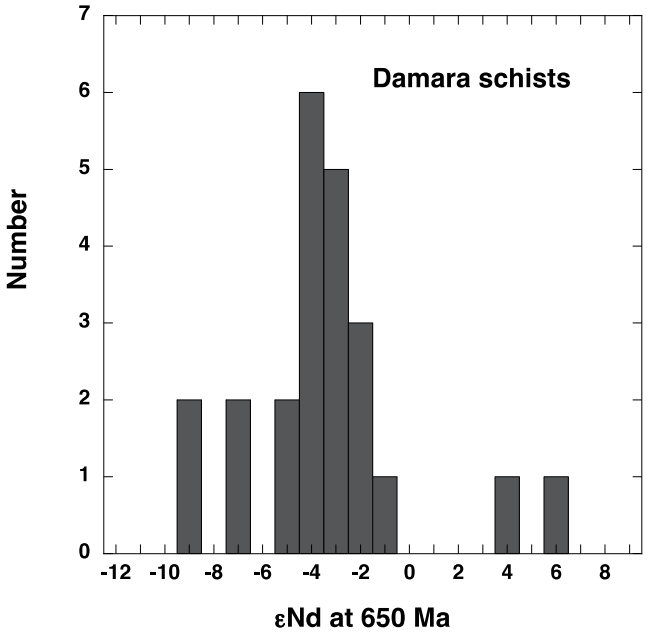

Group-2 plutons are dominated by A-type granites that are syn- to post-tectonic (525–486 Ma) [116–118]. Sr and Nd isotope signatures are less evolved than the S-types ($^{87}Sr/^{86}Sr$ 0.7034–0.709, εNd 0 to −6, as low as −16 for the Sorris Sorris A-type); $\delta^{18}O$ is high (10‰–13‰). Generation of these hot (>800 °C) A-type magmas likely resulted from partial melting of a deep-seated (8–10 kb) tonalitic source, perhaps initiated by mantle-derived magmas, followed by extensive differentiation.

Group-3 includes I-type, metaluminous, hornblende (+/−clinopyroxene) diorite to granodiorite plutons that make up about 2% of the exposed granitoids. Isotopic signatures for this group vary widely ($^{87}Sr/^{86}Sr$ 0.704–0.713, εNd 0 to −20, $\delta^{18}O$ 7‰–13‰), suggesting a range of magma sources

that assimilated crust [90,111,112,119–121]. Titanite and zircon U–Pb ages of 555–540 Ma indicate the I-type suite comprises the oldest intrusive rocks within the Damara Orogen and were emplaced coeval with the onset of high-grade metamorphism [99,122]. A distinct suite of *ca.* 540 Ma syenites (with a more limited range of Sr–Nd isotopic ratios [123]) was also emplaced at that time. The dioritic rocks with more primitive Sr–Nd–O isotope signatures [119] may have been derived from the mantle with limited crustal assimilation, or be partial melts of mafic lower crustal intrusions of early Pan-African age [122]. Those with very low initial εNd and high Sr/Y ratios (Goas and Okongava in the Central Zone) may represent partial melts of Archean-Proterozoic mafic lower crust.

The thermal conditions of continent-continent collision, high heat production in Damara metasediments [124] and high fertility of the crust combined to produce massive mid/lower crustal melting in the Damara Orogen. The dominance of S-type granites and the absence of clearly mantle-like isotopic signatures indicate the importance of crustal recycling rather than juvenile additions during the Damara Orogeny [114,115]. It is possible, however, that the widespread magmatism and high-T metamorphism was ultimately the result of primitive magma emplaced at deeper crustal levels. Pervasive crustal melting would have established a density filter preventing further ascent of mafic magmas, and would greatly increase the chance of hybrid magmas forming in the middle crust at the present level of exposure. The small volume of I-type granitoids does not, therefore, rule out greater mantle contributions at depth.

Tectonic Evolution

Rifting of the Congo and Kalahari cratons from Rodinia occurred between 800 and 700 Ma [89,125]. Extension produced rhyolitic volcanic complexes at about 750 Ma [98,126]. Development of an oceanic spreading center and growth of Khomas oceanic crust occurred by about 700 Ma [89]. A significant part of the Khomas Ocean was floored by oceanic lithosphere that closed by subduction beneath the Congo craton between 570 and 540 Ma [4,89–91,103,125,127]. Basement cored gneiss domes and isotopic signatures in the granitoids indicate attenuated Congo continental crust in the part of the Khomas Ocean basin that now comprises the Central zone, but the Southern zone almost certainly was underlain by oceanic crust. This combination of oceanic and attenuated continental lithosphere suggests a setting similar to the present Japan Sea [30].

Closure of the Khomas Ocean involved high-angle convergence with overthrusting at both margins (Figure 17). The distinct metamorphic zonation of the Inland branch, with Barrovian metamorphism on the orogen flanks, reflects structural thickening at the craton margins, while Andean- or Cordilleran-style low-P/high-T metamorphic conditions in the Central zone and accretionary prism-like features of the Southern zone Kuiseb schist [90], and early calcalkaline magmatism reflect subduction beneath this zone [103,128]. The Matchless amphibolite belt is a thrust slice of oceanic crust incorporated within the accretionary wedge, immediately above (north) of the suture at the Uis Pass Line. Past arguments against subduction related closure of the Khomas Ocean have been based on granite geochemistry [129], and the apparent lack of blueschists and eclogites [130]; high-P metamorphic rocks, however, are exposed to the east along strike in the suture zone [131,132].

Figure 17. Tectonic evolution diagrams for the Damara Belt of the Damara Orogen (modified from Barnes and Sawyer [4]).

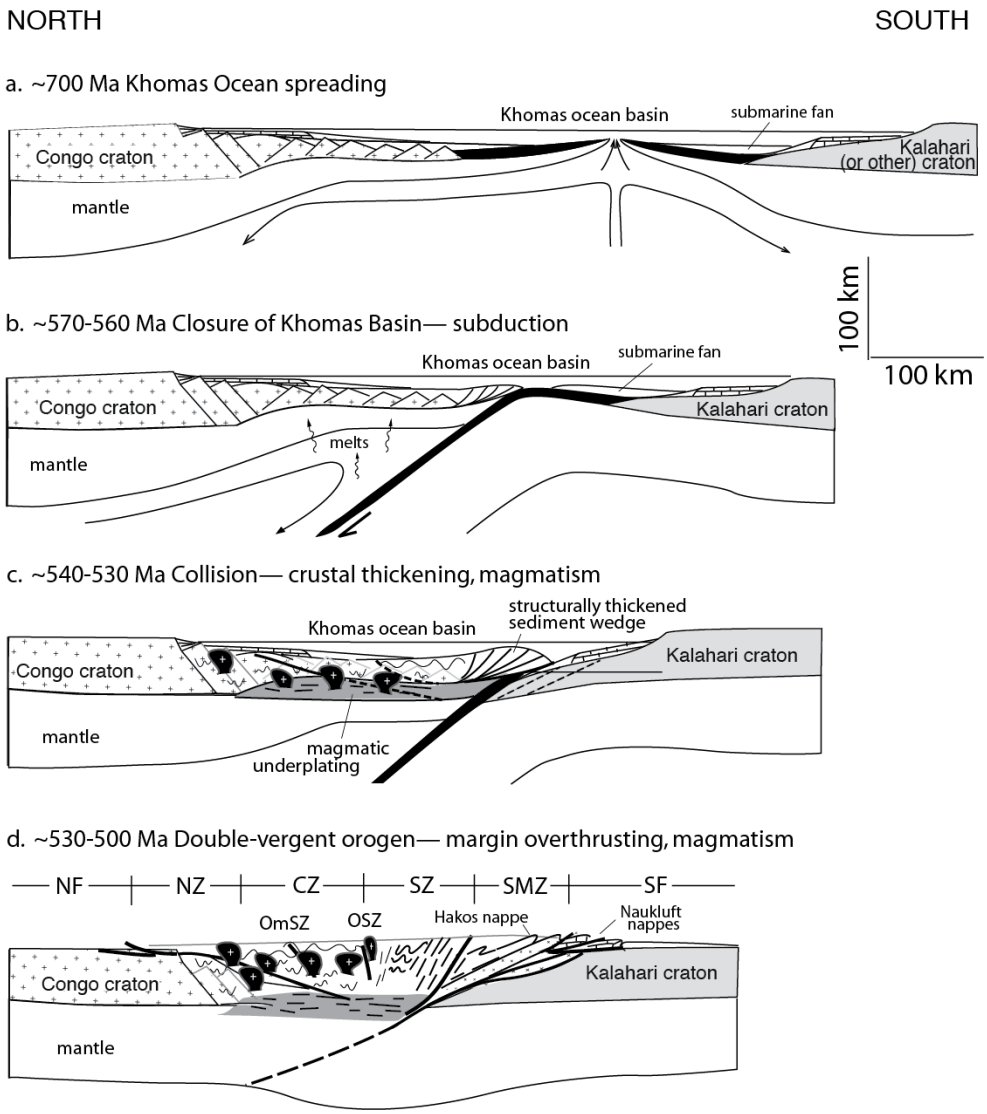

3. Processes of Accretion in Turbidite-Dominated Orogens

Crustal accretion in the Rangitatan, Lachlan, and Damara Orogens involved deformation of submarine turbidite fans and the underlying oceanic basement resulting in shortening (>50%) and crustal thickening. Deformed turbidites now occur either as belts of thrust-imbricated, upright chevron-folded, low-grade turbidites, or zones of higher grade metasedimentary rocks that are characterized by homoclinally dipping schistosity and transposition layering. In these three Phanerozoic examples turbidite deformation resulted from accretion of intra-oceanic plateau (Chatham Rise for the Rangitatan Orogen), convergent margin tectonism driven by closure of marginal (back-arc) basins (western Lachlan Orogen), and closure of an ocean basin by convergence between continents (Damara Orogen). The accreted turbidite fans are a common feature, but each orogen has a unique style or crustal architecture tied to the specific tectonic setting and the position of the turbidites with respect to plate-scale tectonic elements. The Rangitatan, Lachlan, and Damara orogens show that parameters such as the thickness, structural style, metamorphic history, and tectonic position of the

former submarine fan, as well as the age and nature of the underlying basement, are all important variables for interpreting crustal evolution.

3.1. Settings of Turbidites

In most orogens, tectonic reconstructions are based on recognition and interpretations of key geologic or tectonic elements, as well as the structural architecture and tectonic vergence defined by fault/shear zone dips, the distribution of rock types, and the temporal and spatial distributions of metamorphism and magmatism (for example Gray and Foster [8,19] for the Lachlan Orogen; Mortimer [5], for the Rakaia Wedge). The thickness of the turbidite successions and the degree of shortening (>50%) and thickening (up to 300%) support an oceanic depositional setting (Figure 18).

Figure 18. Cross sections showing two end-members of continental crust formation from deformed turbidite fans on oceanic crust. The Lachlan-style (**a**) starts as a thick turbidite fan deposited on mafic back-arc-basin crust. When the marginal basin closes, imbricated basaltic crust forms most of the lower crust and deformed sediments and felsic syn- to post-tectonic plutons form the upper crust; The Rakaia-style (**b**) starts with a large sediment fan deposited on oceanic crust or an ocean plateau. A layered crust of continental thickness is formed when the turbidite fan is shorted and metamorphosed as it enters a subduction zone. The lower crust is composed of thickened mafic crust.

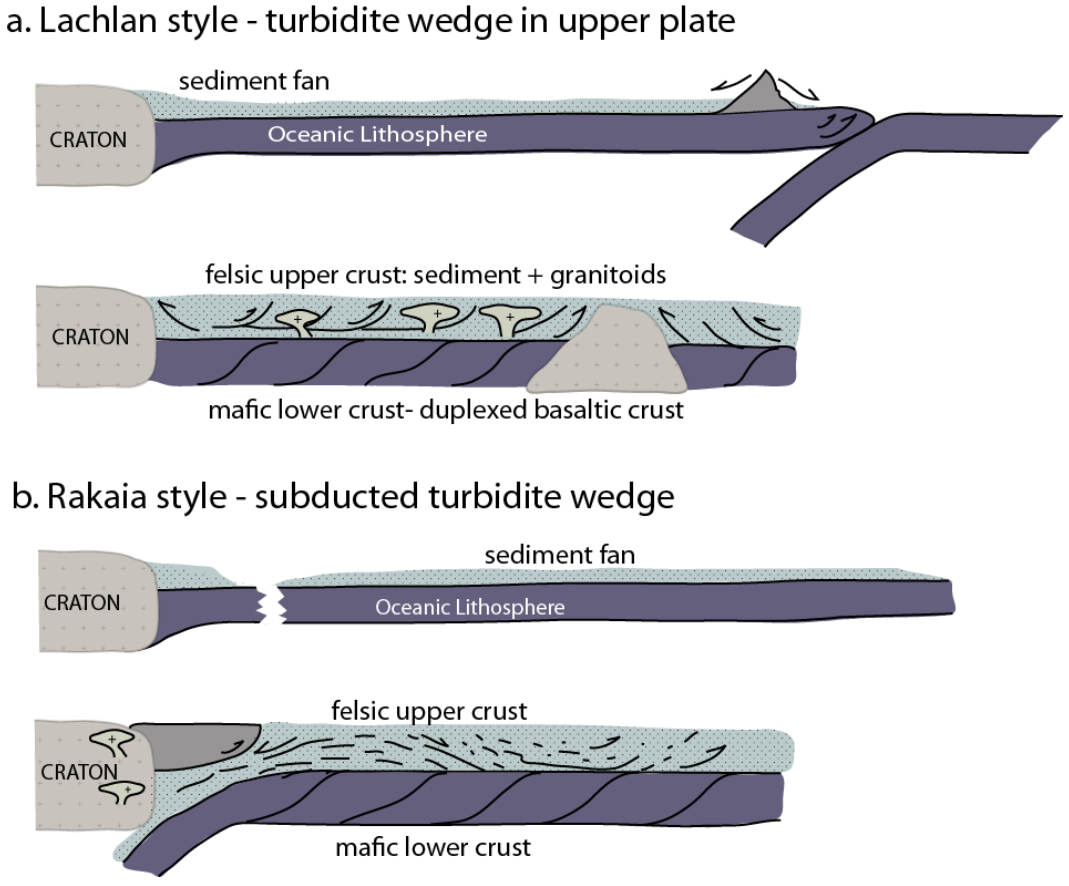

The Lachlan Orogen has extensive turbidites, extending over a 750 km width, thrust systems of mixed vergence, and a central high-T/low-P metamorphic complex. There are certain characteristics of

the Lachlan Orogen that are important for any tectonic reconstruction [19]. These include: (1) Three simultaneously operating oceanic thrust systems in different parts of a marginal ocean basin that was behind a long-lived, outboard subduction system along the eastern margin of Gondwana; (2) Blueschist blocks in serpentinite-matrix mélanges along major faults in the western and central Lachlan; (3) Mélange and broken formations along faults within the frontal fault system of the central Lachlan; (4) Discordant post-tectonic granitoids in the western Lachlan and large elongate composite granitoid batholithes in the central and eastern Lachlan; (5) Shear zone bounded low-P/high-T metamorphic complexes with regional aureole-style metamorphism related to S-type granites. These features are consistent with accretion in the Lachlan Orogen resulting from thickening and imbrication of thick submarine fans and the underlying oceanic lithosphere, in a "Woodlark basin style" double divergent, convergent system [2].

The Lachlan turbidite fans developed on back-arc-basin lithosphere [18,57] analogous to the Phillippine Sea or Japan Sea [19]. Each of these two modern analogues contains different tectonic elements within the basin that would influence deformational styles when they close in the future, including: microcontinental ribbons (e.g., Tasmania [133]) in the former, and relict arcs (e.g., the Cambrian Licola arc [22,32], and Ordovician Macquari arc [38]). The ribbon continents and arcs provide significant rigidity contrasts to the basaltic back-arc basing crust during crustal shortening and thickening, which may explain the three different accretionary thrust belts in the Lachlan.

For the Damara Orogen the accretionary prism-like nature of the Southern zone schists [89,90] as well as their strong similarities to those of the Otago Schist belt in New Zealand [66] suggest that this orogen is another example of continental growth by subduction-accretion of turbidites deposited on oceanic lithosphere.

The Rangitatan Orogen of New Zealand provides the least complicated setting. Representing part of the Mesozoic convergent margin of Gondwana facing a large ocean basin, the Rangitatan Orogen evolved in a forearc position typical of the modern day Aleutian arc-subduction complex with a turbidite fan accreted via underthrusting [134,135].

3.2. Significance of Sediment fan Thickness and Timing

Other parameters that affect accretionary orogen development include the thickness of the turbidite fan, the relative depositional age of the fan, the timing of fan shortening and thickening, and the age of the oceanic lithosphere relative to basin closure [30].

For the Lachlan Orogen, the age of back-arc basin crust is 505–495 Ma, most of the submarine fan system developed between 490 and 460 Ma, and the deformation that caused the back arc basin closure occurred from ~450 Ma to 410 Ma (*i.e.*, some 50 million years after oceanic lithosphere formation and some 30–20 million years after submarine fan deposition). These conditions favor chevron folding, without the significant stratal disruption and mélange or broken formation typical of shallow levels of modern accretionary complexes [136]. Folding requires lithification or precompaction of the sediment fan and, therefore, time for burial and dewatering on the seafloor before deformation. Metamorphism due to sediment loading occurs in modern submarine fans including the Bengal Fan, and leads to closed system quartz vein formation during shortening, as has been documented in the Lachlan Orogen example [137].

During accretion parts of oceanic lithosphere are incorporated into the accretionary thrust wedge and preserved as fault-bounded slices, with the Matchless amphibolite belt in the Damara Orogen, and the slices of basaltic crust in the western Lachlan Orogen providing an excellent examples. The temperature, and therefore, age of the oceanic lithosphere is important. The western Lachlan Orogen shows that thick, lithified or partially lithified turbidite fans (4–5 km thicknesses) sitting on old, cold oceanic lithosphere produce dominantly chevron-folded, thrust-interleaved packages that incorporate fault-bounded, duplexed slivers of the upper parts of the basaltic back-arc basin oceanic lithosphere. This process is inferred to occur by low-angle underthrusting with the turbidites predominantly deforming in the overriding plate [20,138].

In the case of the Rakaia wedge of New Zealand, the age of the underlying oceanic lithosphere as inferred from the Dun Mountain ophiolite is ~280 Ma [139] with Permian to Triassic submarine fan sedimentation (~280 through 200 Ma [63]), and eventual wedge thickening at 160–150 Ma [66] (*i.e.*, some 120 million years after oceanic lithosphere formation and some 40 million years after fan deposition).

In this respect, plate convergence for significant parts of the Lachlan and the Rakaia wedge of New Zealand involves cold oceanic lithosphere and thick turbidite fans (4–5 km thicknesses), with the deformation of the turbidites in the Rakaia wedge occurring on the down-going slab (Figure 17) [62]. Deformation and metamorphism of the Kuiseb Schist of the Damara belt also occurred on the down-going slab [4,30].

Both the Rangitatan (Otago Schist) and Damara Orogens (Kuiseb Schist) show evidence for coupling between the overriding margin and the subducting slab, with the thick turbidite fan sitting on the subducting plate, producing an intensely deformed, highly thickened wedge that underwent Barrovian metamorphism. In both the Rakaia wedge and Southern zone of the Damara, the wedge underwent significant structural thickening by shear-related, non-coaxial deformation at the subduction interface [5,19] to produce transpositional layering or schistosity and a pronounced rodding lineation (*i.e.*, S-L tectonites). These are the dominant fabrics produced in this subduction interface environment that have been attributed to underplating in a coaxial flattening strain environment [140,141]. In both of these cases, arc magmatism occurs in the overriding plate, but not in the intensely coupled zones. In New Zealand, magmatism occurred on the Gondwana margin side of the Dun Mountain ophiolite and not in the thickened wedge. In the Damara Belt most magmatism occurred in the Central zone and where partial melting occurred within the over thickened Precambrian continental basement. Early dioritic intrusions in the Damara may have been partly subduction generated. Only in the Rakaia wedge were the turbidites not partially melted during subduction and/or tectonic shorting to any significant degree.

3.3. The Template of Accretion

The Rangitatan Lachlan, and Damara orogens provide a disconnected history of the tectonic process of turbidite accretion in the Phanerozoic, and show that there is no uniform template for the accretionary process that adds these density and compositionally stratified sections to the continent. This is reflected in the crustal architecture of each orogen, as well as the temporal and spatial variations in the development of deformation fabrics, metamorphism, and magmatism. The Lachlan Orogen is composed of three thrust belts with contrasting vergence, whereas the Damara Orogen

shows divergent thrust systems, and the Rangitatan Orogen one thrust system and a steeply dipping backstop behind the sediment wedge. Within the orogenic architecture, the spatial variations in types of metamorphism delineate the tectonic setting. To a first order approximation, the high-P/low-T metamorphic rocks (blueschists and eclogites) define the subduction channel, the moderate-high-P/ moderate-T (Barrovian style) metamorphic rocks define the regions of structural thickening above the subduction interface, and the low-P/high-T regional aureole metamorphic rocks intruded by large, elongate composite granitoids define the roots of the magmatic arc.

The Rakaia wedge has relict blueschist metamorphism preserved in intercalated metabasites near the interface between the volcaniclastic trench sediment and the accreted, deformed quartz-rich fan [71], whereas the wedge proper shows Barrovian metamorphism with garnet-oligoclase assemblages in the core of the Otago schist [70]. Similarly, the schistose part of the Damara Orogen shows intermediate-P/ intermediate-T (Barrovian-style) metamorphism [103]. The schistose belt dips towards, but verges away from the Central zone belt of large, syn-tectonic granitoids and high-T metamorphism.

The Lachlan Orogen shows regional low-grade, intermediate-P metamorphism [19], but has two belts of low-P/high-T metamorphism associated with composite batholiths [142]. In the western and central Lachlan, blueschist metamorphism is preserved in fault-bounded lenses-shaped blocks within the serpentinite-matrix mélange of the major faults zones [26,27].

4. Discussion and Conclusions

The three examples provide insight into the possible range of processes involved in basin shortening and turbidite fan thickening: Rangitaton—subduction underthrusting, Lachlan—accretionary wedge thickening, and Damara—wedge thrusting and continental collision (Figure 17). All three represent different relative contributions of crustal growth and crustal recycling. The marked shortening and thickening of the crust and the involvement of predominantly oceanic basement are key factors in recognizing ancient subduction-accretion processes in such orogens. The presence of the lower crustal layer of imbricated oceanic crust coupled with the overlying thickened sedimentary succession, yields a density structure that is remarkably stable, isostatically balanced near sea level [143]. Crustal growth is dominated by the tectonically thickened mafic lower crustal component, which was originally the depositional substrate of the turbidites. On the basis of the published (see references in the Lachlan and Rangitaton sections) and unpublished (Figure 14 for the Damara example [92]) detrital zircon U–Pb age distributions, most of the sediment in the turbide fans is recycled from adjacent continents and arcs (see [144,145] for other examples).

Felsic and mafic magmatism contributes to both crustal growth and chemical differentiation of the crust, both new and pre-existing, by recycling and mixing oceanic and continental crust to different degrees. Synorogenic magmatism in the Lachlan added variable amounts of new crust from the mantle with greater amounts in the A- and I-granitoids based on Lu–Hf and O isotopic data from magmatic zircons and whole rocks [3]. The Median batholith in New Zealand comprises significant new crust either directly from subduction-generated partial melting in an Andean setting, or later by remobilization of the young lower arc crust and formation of adakites [80]. In the Damara, granitic magmatism largely regenerated the crustal stack, most likely because the lower crust in part of the orogen was the thinned edge of the Congo craton. Some of the early dioritic magmatism may have a

primitive component, either because it was derived from the mantle or by partial melting of Neoproterozoic mafic lower crust [122].

Granitic magmatism plays an important role in the differentiation of structurally thickened and accreted turbidite fan systems. Turbidite-dominated orogens tend to be characterized by large volumes of syn- to post-tectonic granite, such as those in all zones of the Lachlan Orogen, and in the Central zone of the Damara Orogen. Turbidites, in particular the more feldspathic (greywacke) and pelitic lithologies, represent fertile sources for crustal melting [146]. There is clear isotopic evidence in both the Lachlan and Damara orogens, for derivation of most of the S-type granites from partial melting of the meta-turbidites or sediment contamination of the I-types. Additional source components are sometimes required to explain the chemical/isotopic constraints, e.g., contributions from underlying Cambrian oceanic crust and syn-magmatic mantle-derived melts (Lachlan Orogen [45,47]), or Precambrian crystalline basement (Damara granitoids [122]).

It is important to recognize the somewhat unique signature of this style of crustal growth and accretion in the long term geological and isotopic record, particularly that estimated from detrital zircons, which are one of the most utilized records of crustal growth through time [147,148]. The mafic oceanic basement that makes up the lower crust represents a major fraction of the continental crustal growth in turbidite-dominated orogens, much of which is never remobilized or directly exposed at the surface. In addition, this crust is generally not zircon-bearing by nature and will not widely be represented in the global detrital zircon U–Pb age record because of the mafic composition and the relatively high density; emplacement in the lower crust means little will be exhumed and eroded. Older Lu–Hf isotopic model ages in younger zircons will reflect the presence of extensive mafic lower crust, but only if partially melted hundreds of millions of years later without mixing with juvenile or continental components [147–152]. Partial melting of the oceanic lower crustal layer some tens of millions of years later will likely not be revealed by detrital zircon Hf isotopic composition because these data will be similar to the signature of juvenile crust. It would appear, rather, that the crustal growth occurred by arc or extensional TTG-like magmatism, when it is actually accretion of the upper part of an ocean or back-arc basin. A similar point could be made for mafic crustal underplates, lower crustal mafic sills, and accreted oceanic plateaus.

Perspectives gained by comparing the three Phanerozoic turbidite orogens may be applied to Archean and Proterozoic belts as templates for helping decipher ancient tectonic settings and geodynamics. Belts like the Mesoarchean Jardine metasedimentary sequence of the Wyoming Province [153] and Proterozoic Colorado-Yavapai provinces of Laurentia [154–156] share some comparable styles of deformation, metamorphism, magmatism, and evolution. The microcosm of features in the Archean Jardine metaturbidites and the relationship with voluminous TTG-style magmatism appears to closely resemble the evolution of the Rangatitatan Orogens in that is was likely deposited adjacent to an older continent on oceanic crust, metamorphosed to lower greenschist facies and deformed by upright chevron folds [153].

Acknowledgments

This research was supported by National Science Foundation Grants EAR0073638, EAR-0440188, and EAR0738874. Our review stems from many years of collaborative research with David R. Gray in these three regions. Interactions with Chris Fergusson, Vince Morand, Clive Willman, Bob Gregory,

Roland Maas, Nick Mortimer, and Paul Mueller have helped shaped our understanding of the topics summarized in this paper.

Conflict of Interest

The authors declare no conflict of interest.

References

1. Patchett, P.J.; Bridgwater, D. Origin of continental crust of 1.9–1.7 Ga age defined by Nd isotopes in the Ketilidian terrain of South Greenland. *Contrib. Miner. Petrol.* **1984**, *87*, 311–318.
2. Foster, D.A.; Gray, D.R. The structure and evolution of the Lachlan Fold Belt (Orogen) of eastern Australia. *Annu. Rev. Earth Plan. Sci.* **2000**, *28*, 47–80.
3. Kemp, A.I.S.; Hawkesworth, C.J.; Collins, W.J.; Cray, C.M.; Blevin, P.L. Isotopic evidence for rapid growth in an extensional accretionary orogeny: The Tasmanides, eastern Australia. *Earth Planet. Sci. Lett.* **2009**, *284*, 455–466.
4. Barnes, S.; Sawyer, E. An alternative model for the Damara mobile belt: Ocean crust subduction and continental convergence. *Precambrian Res.* **1980**, *13*, 297–336.
5. Mortimer, N. New Zealand's geological foundations. *Gondwana Res.* **2004**, *7*, 261–272.
6. Mortimer, N. Jurassic tectonic history of the Otago Schist, New Zealand. *Tectonics* **1993**, *12*, 237–244.
7. Veevers, J.J. *Billion-year Earth History of Australia and Neighbours in Gondwanaland*; GEMOC Press: Sydney, Australia, 2000.
8. Gray, D.R.; Foster, D.A. Regional geology: Tasman Orogen, Australia. *Encycl. Geol.* **2004**, *1*, 237–252.
9. Glen, R.A. The Tasmanides of eastern Australia. *Geol. Soc. Lond. Spec. Publ.* **2005**, *246*, 23–96.
10. Fergusson, C.L.; Coney, P.J. Implications of a Bengal Fan-type deposit in the Paleozoic Lachlan fold belt of southeastern Australia. *Geology* **1992**, *20*, 1047–1049.
11. Powell, C.McA. Tectonic relationship between the late Ordovician and Late Silurian palaeogeographies of southeastern Australia. *J. Geol. Soc. Aust.* **1983**, *30*, 353–373.
12. Vandenberg, A.H.M.; Stewart, I.R. Ordovician terranes of the southeastern Lachlan Fold Belt: Stratigraphy, structure and palaeogeographic reconstruction. *Tectonophysics* **1992**, *214*, 159–176.
13. Gray, C.M.; Webb, J. Provenance of Palaeozoic turbidites in the Lachlan Orogenic Belt: Strontium isotopic evidence. *Aust. J. Earth Sci.* **1995**, *42*, 95–105.
14. Fergusson, C.L.; Fanning, C.M. Late Ordovician stratigraphy, zircon provenance and tectonics, Lachlan Fold Belt, southeastern Australia. *Aust. J. Earth Sci.* **2002**, *49*, 423–436.
15. Turner, S.P.; Kelley, S.P.; VandenBerg, A.H.M.; Foden, J.; Sandiford, M.; Flöttmann, T. Source of the Lachlan fold belt flysch linked to convective removal of the lithospheric mantle and rapid exhumation of the Delamerian-Ross fold belt. *Geology* **1996**, *24*, 941–944.
16. Crawford, A.J.; Keays, R.R. Cambrian greenstone belts in Victoria: Marginal sea crust slices in the Lachlan Fold Belt of southeastern Australia. *Earth Planet. Sci. Lett.* **1978**, *41*, 197–208.
17. Crawford, A.J.; Keays, R.R. Petrogenesis of Victorian Cambrian tholeiites and implications for the origin of associated boninites. *J. Pet.* **1987**, *28*, 1075–1109.

18. Foster, D.A.; Gray, D.R.; Spaggiari, C.; Kamenov, G.; Bierlein, F.P. Palaeozoic Lachlan Orogen, Australia; accretion and construction of continental crust in a marginal ocean setting: Isotopic evidence from Cambrian metavolcanic rocks. *Geol. Soc. Lond. Spec. Publ.* **2009**, *318*, 329–349.
19. Gray, D.R.; Foster, D.A. Tectonic evolution of the Lachlan Orogen, southeast Australia: Historical review, data synthesis and modern perspectives. *Aust. J. Earth Sci.* **2004**, *51*, 773–817.
20. Spaggiari, C.V.; Gray, D.R.; Foster, D.A. Ophiolite accretion in the Lachlan Orogen, southeastern Australia. *J. Struct. Geol.* **2004**, *6*, 87–112.
21. Offler, R.; McKnight, S.; Morand, V. Tectonothermal history of the western Lachlan Fold Belt, Australia: Insights from white mica studies. *J. Metamorph. Geol.* **1998**, *16*, 531–540.
22. Spaggiari, C.V.; Gray, D.R.; Foster, D.A.; McKnight, S. Evolution of the boundary between the western and central Lachlan Orogen: Implications for Tasmanide tectonics. *Aust. J. Earth Sci.* **2003**, *50*, 725–749.
23. Fergusson, C.L. Early Palaeozoic backarc deformation in the Lachlan Fold Belt, southeastern Australia: Implications for terrane translations in eastern Gondwanaland. *Geodyn. Ser.* **1987**, *19*, 39–56.
24. Miller, J.McL.; Gray, D.R. Subduction related deformation and the Narooma anticlinorium, eastern Lachlan Orogen. *Aust. J. Earth Sci.* **1997**, *44*, 237–251.
25. Watson, J.M.; Gray, D.R. Character, extent and significance of broken formation for the Tabberabbera Zone, central Lachlan Orogen. *Aust. J. Earth Sci.* **2001**, *48*, 943–954.
26. Spaggiari, C.V.; Gray, D.R.; Foster, D.A. Blueschist metamorphism during accretion in the Lachlan Orogen, southeastern Australia. *J. Metamorph. Geol.* **2002**, *20*, 711–726.
27. Spaggiari, C.V.; Gray, D.R.; Foster, D.A.; Fanning, C.M. Occurrence and significance of blueschists in the southern Lachlan Orogen. *Aust. J. Earth Sci.* **2002**, *49*, 255–269.
28. Morand, V.J. Low-pressure regional metamorphism in the Omeo Metamorphic Complex, Victoria, Australia. *J. Metamorph. Geol.* **1990**, *8*, 1–12.
29. Collins, W.J.; Hobbs, B.E. What caused the Early Silurian change from mafic to silicic magmatism in the eastern Lachlan Fold Belt? *Aust. J. Earth Sci.* **2001**, *48*, 25–41.
30. Gray, D.R.; Foster, D.A.; Maas, R.; Spaggiari, C.V.; Gregory, R.T.; Goscombe, B.D.; Hoffmann, K.H. Continental growth and recycling by accretion of deformed turbidte fans and remnant ocean basins: Examples from Neoproterozoic and Phanerozoic orogens. *Geol. Soc. Am. Mem.* **2007**, *200*, 63–92.
31. Foster, D.A.; Gray, D.R.; Bucher, M. Chronology of deformation within the turbidite-dominated Lachlan orogen: Implications for the tectonic evolution of eastern Australia and Gondwana. *Tectonics* **1999**, *18*, 452–485.
32. Spaggiari, C.V.; Gray, D.R.; Foster, D.A. Tethyan and Cordilleran-Type Ophiolites of Eastern Australia: implications for the evolution of the Tasmanides. *Geol. Soc. Lond. Spec. Publ.* **2003**, *218*, 517–539.
33. White, A.J.R.; Chappell, B.W. Granitoid types and their distribution in the Lachlan Fold Belt, SE Australia. *Geol. Soc. Am. Mem.* **1983**, *159*, 21–34.
34. Chappell, B.W.; White, A.J.R.; Hine, R. Granite provinces and basement terranes in the Lachlan Fold Belt, southeastern Australia. *Aust. J. Earth Sci.* **1988**, *35*, 505–521.

35. Hine, R.; Williams, I.S.; Chappell, B.W.; White, A.J.R. Contrasts between I- and S-type granitoids of the Kosciusko Batholith. *J. Geol. Soc. Aust.* **1978**, *25*, 219–234.
36. Keay, S.; Steele, D.; Compston, W. Identifying granite sources by SHRIMP U–Pb zircon geochronology: An application to the Lachlan Fold Belt. *Contrib. Miner. Petrol.* **2000**, *137*, 323–341.
37. Glen, R.A.; Walshe, J.L.; Barron, L.M.; Watkins, J.J. Ordovician convergent margin volcanism and tectonism in the Lachlan sector of east Gondwana. *Geology* **1998**, *26*, 751–754.
38. Glen, R.A.; Crawford; A.J.; Percival, I.G.; Barron, L.M. Early Ordovician development of the Macquarie Arc, Lachlan Orogen, New South Wales. *Aust. J. Earth Sci.* **2007**, *54*, 167–179.
39. Price, R.C.; Brown, W.M.; Woolard, C.A. The geology, geochemistry and origin of late-Silurian, high-Si igneous rocks of the upper Murray Valley, NE Victoria. *J. Geol. Soc. Austr.* **1983**, *30*, 443–459.
40. Phillips, G.N.; Wall, V.J.; Clemens, J.C. Petrology of the Strathbogie Batholith—A cordierite-bearing granite. *Can. Miner.* **1981**, *19*, 47–63.
41. Clemens, J.D.; Wall, V.J. Origin and evolution of a peraluminous silicic ignimbrite suite: The Violet Town Volcanics. *Contrib. Miner. Petrol.* **1984**, *88*, 354–371.
42. Rossiter, A.G. Granitic rocks of the Lachlan Gold Belt in Victoria. *Geol. Soc. Aust. Spec. Publ.* **2003**, *23*, 217–237.
43. Collins, W.J.; Beams, S.D.; White, A.J.R.; Chappell, B.W. Nature and origin of A-type granites with particular reference to southeastern Australia. *Contrib. Miner. Petrol.* **1982**, *80*, 189–200.
44. McCulloch, M.T.; Chappell, B.W. Nd isotopic characteristics of S- and I-type granites. *Earth Planet. Sci. Lett.* **1982**, *58*, 51–64.
45. Keay, S.; Collins, W.J.; McCulloch, M.T. A three-component isotopic mixing model for granitoid genesis, Lachlan fold belt, eastern Australia. *Geology* **1997**, *25*, 307–310.
46. Adams, C.J.; Pankhurst, R.J.; Maas, R.; Millar, I.L. Nd and Sr isotopic signatures of metasedimentary terranes around the South Pacific margin, and implications for their provenance. *Geol. Soc. Lond. Spec. Publ.* **2005**, *246*, 113–142.
47. Kemp, A.I.S.; Hawkesworth, C.J.; Foster, G.L.; Paterson, B.A.; Woodhead, J.D.; Hergt, J.M.; Gray, C.M. Magmatic and crustal differentiation history of granitic rocks from Hf–O Isotopes in zircon. *Science* **2007**, *315*, 980–983.
48. Williams, I.S. Some observations on the use of zircon U–Pb geochronology in the study of granitic rocks. *Trans. R. Soc. Ed.* **1992**, *83*, 447–458.
49. Bierlein, F.P.; Hughes, M.; Dunphy, J.; McKnight, S.; Reynolds, P.; Waldron, H. Tectonic and economic implications of trace element, $^{40}Ar/^{39}Ar$ and Sm–Nd data from mafic dykes associated with orogenic gold mineralisation in central Victoria, Australia. *Lithos* **2001**, *18*, 1–31.
50. Maas, R.; Nicholls, I.A.; Greig, A.; Nemchin, A. U–Pb zircon studies of mid-crustal metasedimentary enclaves from the S-type Deddick Granodiorite, Lachlan Fold Belt, SE Australia. *J. Pet.* **2001**, *42*, 1429–1448.
51. Soesoo, A.; Bons, P.D.; Gray, D.R.; Foster, D.A. Divergent double subduction: Tectonic and petrologic consequences. *Geology* **1997**, *25*, 755–758.

52. Soesoo, A.; Nicholls, I.A. Mafic rocks spatially associated with Devonian felsic intrusions of the southern Lachlan Fold Belt: A possible mantle contribution to crustal evolution processes. *Aust. J. Earth Sci.* **1999**, *46*, 725–734.
53. Gray, C.M. An isotopic mixing model for the origin of granitic rocks in southeastern Australia. *Earth Plan. Sci. Lett.* **1984**, *70*, 47–60.
54. Gray, C.M. A strontium isotopic traverse across the granitic rocks of southeastern Australia: Petrogenetic and tectonic implications. *Aust. J. Earth Sci.* **1990**, *37*, 331–349.
55. Collins, W.J. Lachlan Fold Belt granitoids: Products of three-component mixing. *Trans. R. Soc. Ed. Earth Sci.* **1996**, *87*, 171–182.
56. Collins, W.J. Evaluation of petrogenetic models for Lachlan Fold Belt granitoids: Implications for crustal architecture and tectonic models. *Aust. J. Earth Sci.* **1998**, *45*, 483–500.
57. Foster, D.A.; Gray, D.R.; Spaggiari, C.V. Timing of subduction and exhumation along the Cambrian East Gondwana margin, and the formation of Paleozoic back-arc basins. *Geol. Soc. Am. Bull.* **2005**, *117*, 105–116.
58. Foster, D.A.; Gray, D.R. Paleozoic crustal growth, structure, strain rate, and metallogeny in the Lachlan Orogen, Eastern Australia. *Ariz Geol. Soc. Dig.* **2008**, *22*, 213–225.
59. Gray, D.R.; Foster, D.A.; Bucher, M. Recognition and definition of orogenic events in the Lachlan Fold Belt. *Aust. J. Earth Sci.* **1997**, *44*, 489–581.
60. Spaggiari, C.V.; Gray, D.R.; Foster, D.A. Lachlan Orogen subduction-accretion systematics revisited. *Austr. J. Earth Sci.* **2004**, *51*, 549–553.
61. Collins, W.J. Nature of extensional accretionary orogens. *Tectonics* **2002**, *21*, 1024–1036.
62. Coombs, D.S.; Landis, C.A.; Norris, R.J.; Sinton, J.M.; Borns, D.J.; Craw, D. The Dun Mountain Ophiolite belt, New Zealand, its tectonic setting, constitution, and origin, with special reference to the southern portion. *Am. J. Sci.* **1976**, *276*, 561–603.
63. Bradshaw, J.D. Cretaceous geotectonic patterns in the New Zealand region. *Tectonics* **1989**, *8*, 803–820.
64. Adams, C.J.; Barley, M.E.; Fletcher, I.R.; Pickard, A.L. Evidence from U–Pb zircon and $^{40}Ar/^{39}Ar$ muscovite detrital mineral ages in metasandstones for movement of the Torlesse suspect terrane around the eastern margin of Gondwanaland. *Terra Nova* **1998**, *10*, 183–189.
65. Adams, C.J.; Cambell, H.J.; Griffin, W.L. Provenance comparisons of Permian to Jurassic tectostratigraphic terranes in New Zealand: Perspectives from detrital zircon age patterns. *Geol. Mag.* **2007**, *144*, 701–729.
66. Gray, D.R.; Foster, D.A. $^{40}Ar/^{39}Ar$ thermochronologic constraints on deformation, metamorphism and cooling/exhumation of a Mesozoic accretionary wedge, Otago Schist, New Zealand. *Tectonophysics* **2004**, *385*, 181–210.
67. Mortimer, N.; Davey, F.J.; Melhush, A.; Yu, J.; Godfrey, N.J. Geological interpretation of a deep crustal seismic reflection profile across the eastern Province and Median Batholith, New Zealand: Crustal architecture of an extended Phanerozoic convergent orogeny. *N. Z. J. Geol. Geophys.* **2003**, *45*, 349–363.
68. Cawood, P.A. Stratigraphic and structural relations of strata enclosing the Dun Mountain ophiolite belt in the Arthurton-Clinton region, Southland. *N. Z. J. Geol. Geophys.* **1987**, *30*, 19–36.

69. Norris, R.J.; Craw, D. Aspiring terrane: an oceanic assemblage from New Zealand and its implications for Mesozoic terrane accretion in the southwest Pacific. *Am. Geophys. Union Geodyn. Ser.* **1987**, *19*, 169–177.
70. Mortimer, N. Metamorphic discontinuities in orogenic belts: Example of garnet–biotite–albite zone in the Otago Schist, New Zealand. *Int. J. Earth Sci.* **2000**, *89*, 295–306.
71. Yardley, B.W.D. The early metamorphic history of the Haast Schists and related rocks of New Zealand. *Contrib. Miner. Petrol.* **1982**, *81*, 317–327.
72. Mortimer, N.; Tulloch, A.J.; Spark, R.N.; Walker, N.W.; Ladley, E.; Allibone, A.; Kimbrough, D.L. Overview of the Median Batholith, New Zealand: A new interpretation of the geology of the Median Tectonic Zone and adjacent rocks. *J. Afr. Earth Sci.* **1999**, *29*, 259–270.
73. Kimbrough, D.L.; Tulloch, A.J.; Geary, E.; Coombs, D.S.; Mattinson, J.M. Isotopic ages from the Nelson region of the South Island, New Zealand: Crustal structure and definition of the Median Tectonic Zone. *Tectonophysics* **1993**, *225*, 433–448.
74. Kimbrough, D.L.; Tulloch, A.J.; Coombs, D.S.; Landis, C.A.; Johnston, M.R.; Mattison, J.M. Uranium-lead ages from the Median Tectonic Zone, South Island New Zealand. *N. Z. J. Geol. Geophys.* **1994**, *37*, 393–419.
75. Muir, R.J.; Ireland, T.R.; Weaver, S.D.; Bradshaw, J.D.; Evans, J.A.; Eby, G.N.; Shelley, D. Geochronology and geochemistry of a Mesozoic magmatic arc system, Fiordland, New Zealand. *J. Geol. Soc. Lond.* **1998**, *155*, 1037–1053.
76. Mortimer, N.; Gans, P.; Calvert, A.; Walker, N. Geology and thermochronometry of the east edge of the Median Batholith (Median Tectonic Zone): A new perspective on Permian to Cretaceous crustal growth of New Zealand. *Island Arc* **1999**, *8*, 404–425.
77. McCulloch, M.T.; Bradshaw, J.Y.; Taylor, S.R. Sm–Nd and Rb–Sr isotopic and geochemical systematics in Phanerozoic granulites from Fiordland, southwest New Zealand. *Contrib. Miner. Petrol.* **1987**, *97*, 183–195.
78. Muir, R.J.; Weaver, S.D.; Bradshaw, J.D.; Eby, G.N.; Evans, J.A. The Cretaceous Separation Point Batholith, New Zealand. Granitoid magmas formed by melting of mafic lithosphere. *J. Geol. Soc. Lond.* **1995**, *152*, 689–701.
79. Klepeis, K.A.; Clarke, G.L.; Rushmer, T. Magma transport and coupling between deformation and magmatism in the continental lithosphere. *GSA Today* **2003**, *13*, 4–11.
80. Wandres, A.M.; Bradshaw, J.D. New Zealand tectonostratigraphy and implications from conglomeratic rocks for the configuration of the SW Pacific margin of Gondwana. *Geol. Soc. Lond. Spec. Publ.* **2005**, *246*, 179–216.
81. Tulloch, A.J. Batholiths, plutons and suites: Nomenclature for granitoid rocks of Westland-Nelson, New Zealand. *N. Z. J. Geol. Geophys.* **1988**, *31*, 505–509.
82. Waight, T.E.; Weaver, S.D.; Muir, J.; Maas, R.; Eby, N. The Hohonu Batholith of North Westland, New Zealand: Granitoid compositions controlled by source H_2O contents and generated during tectonic transition. *Contrib. Miner. Petrol.* **1998**, *130*, 225–239.
83. Tulloch, A.J.; Kimbrough, D.L. The Paparoa Metamorphic Core Complex, New Zealand: Cretaceous extension associated with fragmentation of the Pacific margin of Gondwana. *Tectonics* **1989**, *8*, 1217–1234.

84. Waight, T.E.; Weaver, S.D.; Muir, R.J. Mid-Cretaceous granitic magmatism dating the transition from subduction to extension in southern New Zealand: A chemical and tectonic synthesis. *Lithos* **1998**, *45*, 469–482.
85. Roser, B.; Cooper, A.F. Geochemistry and terrane affiliation of Haast Schist from the western Southern Alps, New Zealand. *N. Z. J. Geol. Geophys.* **1990**, *94*, 635–650.
86. Prave, A.R. Tale of three cratons: Tectostratigraphic anatomy of the Damara Orogen in northwestern Namibia and the assembly of Gondwana. *Geology* **1996**, *24*, 1115–1118.
87. Martin, H.; Porada, H. The intracratonic branch of the Damara Orogen in South West Africa: I. Discussion of Geodynamic models. *Precambrian Res.* **1977**, *5*, 311–338.
88. Hoffmann, K.-H. Lithostratigraphy and facies of the Swakop Group of the southern Damara belt, SWA/Namibia. *Geol. Soc. S. Afr. Spec. Publ.* **1983**, *11*, 43–63.
89. Miller, R.McL. The Pan-African Damara orogen of South West Namibia/Africa. *Geol. Soc. S. Afr. Spec. Publ.* **1983**, *11*, 431–515.
90. Kukla, P.A.; Stanistreet, I.G. Record of the Damaran Khomas Hochland accretionary prism in central Namibia: Refutation of an "ensialic" origin of a Late Proterozoic orogenic belt. *Geology* **1991**, *19*, 473–476.
91. Gray, D.R.; Foster, D.A.; Goscombe, B.; Passchier, C.W.; Trouw, R.A.J. $^{40}Ar/^{39}Ar$ thermochronology of the Pan-African Damara Orogen, Namibia with implications for tectonothermal and geodynamic evolution. *Precambrian Res.* **2006**, *150*, 49–72.
92. Foster, D.A.; Goscombe, B.D.; Newstead, B.L.; Muvangua, E.; Mueller, P.A.; Mapani, B. Rodinia-Gondwana supercontinent cycle refined by detrital zircons from the Damara Orogen. In Proceedings of 2012 Geological Society of America Annual Meeting, Charlotte, NC, USA, 4–7 November 2012; p. 175.
93. Barnes, S. Pan-African serpentinites in central south west Africa/Namibia and the chemical classification of serpentinites. *Geol. Soc. S. Afr. Spec. Publ.* **1983**, *11*, 147–155.
94. Schmidt, A.; Wedepohl, K.H. Chemical composition and genetic relations of the Matchless Amphibolite (Damara Orogenic Belt). *Geol. Soc. S. Afr. Spec. Publ.* **1983**, *11*, 139–145.
95. Killick, A.M. The Matchless Belt and associated sulphide mineral deposits, Damara Orogen, Namibia. *Commun. Geol. Surv. Namib.* **2000**, *12*, 73–80.
96. Kisters, A.F.M.; Jordaan, L.S.; Neumaier, K. Thrust-related dome structures in the Karibib district and the origin of orthogonal fabric domains in the south Central Zone of the Pan-African Damara belt, Namibia. *Precambrian Res.* **2004**, *133*, 283–303.
97. Jacob, R.E.; Moore, J.M.; Armstrong, R.A. Zircon and titanite age determinations from igneous rocks in the Karibib District, Namibia; implications for Navachab vein-style gold mineralization. *Commun. Geol. Surv. Namib.* **2000**, *12*, 157–166.
98. De Kock, G.S.; Eglington, B.; Armstrong, R.A.; Hermer, R.E.; Walraven, F. U–Pb and Pb–Pb ages of the Naauwpoort Rhyolite, Kawakeup leptite and Okongava Diorite: Implications for the onset of rifting and of orogenesis in the Damara Belt, Namibia. *Commun. Geol. Surv. Namib.* **2000**, *12*, 81–88.
99. Jung, S.; Mezger, K. U–Pb garnet chronometry in high-grade rocks; case studies from the central Damara Orogen (Namibia) and implications for the interpretation of Sm–Nd garnet ages and the role of high U–Th inclusions. *Contrib. Miner. Petrol.* **2003**, *146*, 382–396.

100. Jung, S.; Mezger, K. Petrology of basement-dominated terranes. I: Regional metamorphic T-t path from U–Pb monazite and Sm–Nd garnet geochronology (central Damara Orogen, Namibia). *Chem. Geol.* **2003**, *198*, 223–247.
101. Schmitt, R.S.; Trouw, R.A.J.; Passchier, C.W.; Medeiros, S.R.; Armstrong, R. 530 Ma syntectonic syenites and granites in NW Namibia—Their relation with collision along the junction of the Damara and Kaoko belts. *Gondwana Res.* **2012**, *21*, 362–377.
102. Longridge, L.; Gibson, R.L.; Kinnaird, J.A.; Armstrong, R.A. Constraining the timing of deformation in the southwestern Central Zone of the Damara Belt, Namibia. *Geol. Soc. Lond. Spec. Publ.* **2011**, *357*, 107–135.
103. Kasch, K.W.; Regional, P.-T. variations in the Damara Orogen with particular reference to early high-pressure metamorphism along the southern margin. *Geol. Soc. S. Afr. Spec. Publ.* **1983**, *11*, 243–253.
104. Kukla, C. *Strontium Isotope Heterogeneities in Amphibolite Facies, Banded Metasediments—A Case Study from the Late Proterozoic Kuiseb Formation of the Southern Damara Orogen, Central Namibia*; Memoir (Geological Survey (Namibia) 15; Ministry of Mines and Energy, Geological Survey of Namibia: Windhoek, Namibia, 1993; p. 39.
105. Coward, M.P. The tectonic history of the Damaran Belt. *Geol. Soc. S. Afr. Spec. Publ.* **1983**, *11*, 409–421.
106. Swart, R. *The Sedimentology of the Zerrissene Turbidite System, Damara Orogen, Namibia*; Ministry of Mines and Energy, Geological Survey of Namibia: Windhoek, Namibia, 1992.
107. Passchier, C.W.; Trouw, R.A.; Ribeiro, A.; Pacuillo, F.V.P. Tectonic evolution of the southern Kaoko Belt, Namibia. *J. Afr. Earth Sci.* **2002**, *35*, 61–75.
108. Goscombe, B.; Gray, D.R.; Hand, M. Variation in metamorphic style along the northern margin of the Damara Orogen, Namibia. *J. Pet.* **2004**, *45*, 1261–1295.
109. Jung, S. High-temperature, mid-pressure clockwise P-T paths and melting in the development of regional migmatites: The role of crustal thickening and repeated plutonism. *Geol. J.* **2000**, *35*, 345–359.
110. Masberg, P. Garnet-growth in medium-pressure granulite facies metapelites from the central Damara Orogen: Igneous versus metamorphic history. *Commun. Geol. Surv. Namib.* **2000**, *12*, 115–124.
111. McDermott, F.; Harris, N.B.W.; Hawkesworth, C.J. Geochemical constraints on crustal anatexis: A case study from the Pan-African granitoids of Namibia. *Contrib. Miner. Petrol.* **1996**, *123*, 406–423.
112. Haack, U.; Hoefs, J.; Gohn, E. Constraints on the origin of Damaran granites by Rb/Sr and $\delta^{18}O$ data. *Contrib. Miner. Petrol.* **1982**, *79*, 279–289.
113. Jung, S.; Mezger, K.; Hoernes, S. Trace element and isotopic (Sr, Nd, Pb, O) arguments for a mid-crustal origin of Pan-African garnet-bearing S-type granites from the Damara orogen (Namibia). *Precambrian Res.* **2001**, *110*, 325–355.
114. Jung, S.; Mezger, K.; Hoernes, S. Petrology of basement-dominated terranes. II: Contrasting isotopic (Sr, Nd, Pb, O) signatures of basement-derived granites and constraints on the source region of granite (Damara orogen, Namibia). *Chem. Geol.* **2003**, *199*, 1–28.

115. McDermott, F.; Hawkesworth, C.J. Intracrustal recycling and upper-mantle evolution: A case study from the Pan-African Damara mobile belt, central Namibia. *Chem. Geol.* **1990**, *83*, 263–280.
116. Jung, S.; Hoernes, S.; Mezger, K. Geochronology and petrogenesis of Pan-African syn-tectonic S-type and post-tectonic A-type granite (Namibia)—Products of melting of crustal sources, fractional crystallization and wall rock entrainment. *Lithos* **2000**, *50*, 259–287.
117. Jung, S.; Mezger, K.; Hoernes, S. Petrology and geochemistry of syn- to post-collisional metaluminous A-type granites—A major and trace element and Nd–Sr–Pb–O isotope study from the Proterozoic Damara Belt, Namibia. *Lithos* **1998**, *45*, 147–175.
118. McDermott, F.; Harri, N.B.W.; Hawkesworth, C.J. Geochemical constraints on the petrogenesis of Pan-African A-type granites in the Damara Belt, Namibia. *Commun. Geol. Surv. Namib.* **2000**, *12*, 139–148.
119. Hawkesworth, C.J.; Kramers, J.D.; Miller, R.M.G. Old model Nd ages in Namibian Pan-African rocks. *Nature* **1981**, *289*, 278–282.
120. Jung, S.; Hoernes, S.; Mezger, K. Synorogenic melting of mafic lower crust; constraints from geochronology, petrology and Sr, Nd, Pb and O isotope geochemistry of quartz diorites (Damara Orogen, Namibia). *Contrib. Miner. Petrol.* **2002**, *143*, 551–566.
121. Van de Flierdt, T.; Hoernes, S.; Jung, S.; Masberg, P.; Hoffer, E.; Schaltegger, U.; Friedrichsen, H. Lower crustal melting and the role of open-system processes in the generation of syn-orogenic quartz diorite-granite-leucogranite associations: constraints from Sr–Nd–O isotopes from the Bandombaai Complex, Namibia. *Lithos* **2003**, *67*, 205–226.
122. Jung, S.; Masberg, P.; Mihm, D.; Hoernes, S. Partial melting of diverse crustal sources—Constraints from Sr–Nd–O isotopic compositions of quartz diorite-granodiorite-leucogranite associations (Kaoko Belt, Namibia). *Lithos* **2009**, *111*, 236–251.
123. Jung, S.; Mezger, K.; Hoernes, S. Geochemical and isotopic studies of syenites from the Proterozoic Damara Belt (Namibia): Implications for the origin of syenites. *Miner. Mag.* **1998**, *62*, 729–730.
124. Haack, U.; Gohn, E.; Hartmann, O. Radiogenic heat generation in Damaran rocks. *Geol. Surv. S. Afr. Spec. Publ.* **1983**, *11*, 225–232.
125. Gray, D.R.; Foster, D.A.; Meert, J.G.; Goscombe, B.D; Armstrong, R.; Trouw, R.A.J; Passchier, C.W. A Damara Orogen perspective on the assembly of southwestern Gondwana. *Geol. Soc. Lond. Spec. Publ.* **2008**, *294*, 257–278.
126. Hoffman, P.F.; Hawkins, D.P.; Isachsen, C.E.; Bowring, S.A. Precise U–Pb zircon ages for early Damaran magmatism in the Summas Mountains and Welwitschia Inlier, northern Damara belt, Namibia. *Commun. Geol. Sur. Namib.* **1996**, *11*, 47–52.
127. De Kock, G. Forearc basin evolution in the Pan-African Damara Belt, central Namibia: The Hureb Formation of the Khomas Zone. *Precambrian Res.* **1992**, *57*, 169–194.
128. Maloof, A.C. Superposed folding at the junction of the inland and coastal belts, Damara Orogen, Namibia. *Commun. Geol. Sur. Namib.* **2000**, *12*, 89–98.
129. Hawkesworth, C.J.; Gledhill, A.R.; Roddick, J.C.; Miller, R.McG.; Kröner, A. Rb–Sr and $^{40}Ar/^{39}Ar$ studies bearing on models for the thermal evolution of the Damara Belt, Namibia. *Geol. Soc. S. Afr. Spec. Publ.* **1983**, *11*, 323–338.

130. Kröner, A. Rb–Sr geochronology and tectonic evolution of the Pan African belt of Namibia, southwestern Africa. *Am. J. Sci.* **1982**, *282*, 1471–1507.
131. John, T.; Schenk, V. Partial eclogitisation of gabbroic rocks in a late Precambrian subduction zone (Zambia); prograde metamorphism triggered by fluid infiltration. *Contrib. Miner. Petrol.* **2003**, *146*, 174–191.
132. John, T.; Schenk, V.; Haase, K.; Scherer, E.; Tembo, F. Evidence for a Neoproterozoic ocean in south-central Africa from mid-oceanic-ridge-type geochemical signatures and pressure-temperature estimates of Zambian eclogites. *Geology* **2003**, *31*, 243–246.
133. Moore, D.H.; Betts, P.G.; Hall, H. Towards understanding the early Gondwana margin in southeastern Australia. *Gondwana Res.* **2013**, *23*, 1581–1598.
134. Fuis, G.S.; Plfker, G. Evolution of deep structure along the Trans-Alaska Crustal Transect, Chugach Mountains and Copper River Basin, Southern Alaska. *J. Geophys. Res.* **1991**, *96*, 4229–4253.
135. Finzel, E.S.; Trop, J.M.; Ridgeway, K.D.; Enkelmann, E. Upper plate proxies for flat-slap subduction processes in southern Alaska. *Earth Planet. Sci. Lett.* **2011**, *303*, 348–360.
136. Festa, A.; Dilek, Y.; Pini, G.A.; Codegone, G.; Ogatae, K. Mechanisms and processes of stratal disruption and mixing in the development of mélanges and broken formation: redefining and classifying mélanges. *Tectonophysics* **2012**, *568–569*, 7–24.
137. Gray, D.R.; Gregory, R.T.; Durney, D.W. Rock-Buffered fluid-rock interaction in deformed quartz-rich turbidite sequences, eastern Australia. *J. Geophys. Res.* **1991**, *96*, 19681–19704.
138. Gray, D.R.; Foster, D.A. Character and kinematics of faults within the turbidite-dominated Lachlan Orogen: Implications for tectonic evolution of eastern Australia. *J. Struct. Geol.* **1998**, *20*, 1691–1720.
139. Kimbrough, D.L.; Mattison, J.M.; Coombs, D.S.; Landis, C.A.; Johnston, M.R. Uranium-lead ages for the Dun Mountain Ophiolite belt and Brook Street terrane, South Island, New Zealand. *Geol. Soc. Am. B* **1992**, *104*, 429–443.
140. Lundberg, N.; Reed, D.L. Continental margin tectonics: Forearc process. *Rev. Geophys.* **1991**, *29*, 794–806.
141. Von Huene, R.; Scholl, D.W. Observations at convergent margins concerning sediment subduction, subduction erosion, and the growth of continental crust. *Rev. Geophys.* **1991**, *29*, 279–316.
142. Richards, S.W.; Collins, W.J. The Cooma metamorphic complex, a low-P, high-T (LPHT) regional aureole beneath the Murrumbidgee batholith. *J. Met. Geol.* **2002**, *20*, 119–134.
143. O'Halloran, G.L.; Rey, P. Isostatic constraints on the central Victorian lower crust: implications for the tectonic evolution of the Lachlan fold belt. *Aust. J. Earth Sci.* **1999**, *46*, 633–639.
144. Busby, C. Continental growth at convergent margins facing large ocean basins: A case study from Mesozoic convergent-margin basins of Baja California, Mexico. *Tectonophys* **2004**, *392*, 241–277.
145. Ingersoll, R.V.; Dickinson, W.R.; Graham, S.A. Remnant-ocean submarine fans: Largest sedimentary systems on earth. *Geol. Soc. Am. Spec. Publ.* **2003**, *370*, 191–208.
146. Clemens, J.D.; Vielzeuf, D. Constraints on melting and magma production in the crust. *Earth Planet. Sci. Lett.* **1987**, *86*, 287–306.

147. Condie, K.C.; Bickford, M.E.; Aster, R.C.; Belousova, E.; Scholl, D.W. Episodic zircon ages, Hf isotopic composition, and the preservation rate of continental crust. *Geol. Soc. Am. Bull.* **2011**, *123*, 951–957.
148. Voice, P.J.; Kowalewski, M.; Eriksson, K.A. Quantifying the timing and rate of crustal evolution: Global compilation of radiometrically dated detrital zircon grains. *J. Geol.* **2011**, *119*, 109–126.
149. Kemp, A.I.S.; Hawkesworth, C.J.; Paterson, B.A.; Kinny, P.D. Episodic growth of the Gondwana supercontinent from hafnium and oxygen isotopes in zircon. *Nature* **2006**, *439*, 580–583.
150. Belousova, E.A.; Kostitsyn, Y.A.; Griffin, W.L.; Begg, G.C.; O'Reilly, S.Y.; Pearson, N.J. The growth of the continental crust: Constraints from zircon Hf-isotopic data. *Lithos* **2010**, *119*, 457–466.
151. Iizuka, T.; Komiya, T.; Rino, S.; Maruyama, S.; Hirata, T. Detrital zircon evidence for Hf-isotopic evolution of granitoid crust and continental growth. *Geochem. Cosmochim. Acta* **2012**, *74*, 2450–2472.
152. Foster, D.A.; Mueller, P.A.; Heatherington, A.; Gifford, J.N.; Kalakay, T.J. Lu–Hf systematics of magmatic zircons reveal a Proterozoic crustal boundary under the Cretaceous Pioneer batholith, Montana. *Lithos* **2012**, *142–143*, 216–225.
153. Foster, D.A.; Mueller, P.A.; Goscombe, B.D.; Gray, D.R. Accreted Turbidite Fans and Remnant Ocean Basins in Phanerozoic Orogens: A Template for a Significant Precambrian Crustal Growth and Recycling Process. In *Archean Earth and Early Life*; Dilek, Y., Furnes, H., Eds.; Springer: New York, NY, USA, 2013; in press.
154. Karlstrom, K.E.; Bowring, S.A. Early Proterozoic orogeny assembly of tectonostratigraphic terranes in southwestern North America. *J. Geol.* **1988**, *96*, 561–576.
155. Bickford, M.E.; Hill, B.M. Does the arc accretion model adequately explain the Paleoproterozoic evolution of southern Laurentia? An expanded interpretation. *Geology* **2007**, *35*, 167–170.
156. Condie, K.C. Preservation and recycling of crust during accretionary and collisional phases of Proterozoic orogens: A bumpy road from Nuna to Rodinia. *Geociences* **2013**, *3*, 240–261.